Molecular Biology of the Cell
Vol. 21, 2514–2528, July 15, 2010

The Interferon-γ–induced Murine Guanylate-Binding Protein-2 Inhibits Rac Activation during Cell Spreading on Fibronectin and after Platelet-derived Growth Factor Treatment: Role for Phosphatidylinositol 3-Kinase

Angela F. Messmer-Blust,* Sujata Balasubramanian,* Victoria Y. Gorbacheva,† Jonathan A. Jeyaratnam,* and Deborah J. Vestal*†

*Department of Biological Sciences, University of Toledo, Toledo, OH 43606; and †Department of Molecular Biology of the Lerner Research Institute, Cleveland Clinic Foundation, Cleveland, OH 44195

Submitted April 30, 2009; Revised May 14, 2010; Accepted May 17, 2010
Monitoring Editor: Josephine Adams

Exposure of cells to certain cytokines can alter how these same cells respond to later cues from other agents, such as extracellular matrix or growth factors. Interferon (IFN)-γ pre-exposure inhibits the spreading of fibroblasts on fibronectin. Expression of the IFN-γ–induced GTPase murine guanylate-binding protein-2 (mGBP-2) can phenocopy this inhibition and small interfering RNA knockdown of mGBP-2 prevents IFN-γ–mediated inhibition of cell spreading. Either IFN-γ treatment or mGBP-2 expression inhibits Rac activation during cell spreading. Rac is required for cell spreading. mGBP-2 also inhibits the activation of Akt during cell spreading on fibronectin. mGBP-2 is incorporated into a protein complex containing the catalytic subunit of phosphatidylinositol 3-kinase (PI3-K), p110. The association of mGBP-2 with p110 seems important for the inhibition of cell spreading because S52N mGBP-2, which does not incorporate into the protein complex with p110, is unable to inhibit cell spreading. PI3-K activation during cell spreading on fibronectin was inhibited in the presence of mGBP-2. Both IFN-γ and mGBP-2 also inhibit cell spreading initiated by platelet-derived growth factor treatment, which is also accompanied by inhibition of Rac activation by mGBP-2. This is the first report of a novel mechanism by which IFN-γ can alter how cells respond to subsequent extracellular signals, by the induction of mGBP-2.

INTRODUCTION

The ability of a cell to identify and respond to cues from the extracellular environment provides important points of regulation for many cellular processes, including proliferation, differentiation, adhesion, and migration (Gonzalez-Amaro and Sanchez-Madrid, 1999; Coppolino and Dedhar, 2000). Although much is known about how cells respond to individual cytokines, growth factors, and extracellular matrix (ECM) components, cells within whole organisms are frequently exposed to multiple extracellular signals either sequentially or simultaneously. This exposure to more than one signal is what is believed to occur in environments containing multiple proinflammatory cytokines. Although such an environment is believed to occur frequently, experimentally little is known about how exposure to one signal modulates the subsequent exposure to another.

This article was published online ahead of print in *MBoC in Press* (http://www.molbiolcell.org/cgi/doi/10.1091/mbc.E09–04–0344) on May 26, 2010.

Address correspondence to: Deborah J. Vestal (deborah.vestal@utoledo.edu).

Abbreviations used: ECM, extracellular matrix; FN, fibronectin; GBP, guanylate-binding protein; GST, glutathione transferase; IFN, interferon; IL, interleukin; PAK, p21-activated kinase; PBD, PAK binding domain; PBS, phosphate-buffered saline; PDGF, platelet-derived growth factor; PI3-K, phosphoinositol 3-kinase; PMSF, phenylmethylsulfonyl fluoride; TCL, total cell lysate; TNF, tumor necrosis factor.

Interferon (IFN)-γ is a proinflammatory cytokine frequently found in environments containing other cytokines and growth factors. IFNs have profound and pleiotropic effects on cells. Originally studied for their antiviral and antimicrobial activities, they also have antitumor, antiangiogenic, and proapoptotic effects on some cells (Boehm *et al*., 1997; Der *et al*., 1998; Stark *et al*., 1998). Other consequences of IFN exposure include changes in adhesion (Shaw and Mercurio, 1989; Shaw *et al*., 1990), migration (Adelmann-Grill *et al*., 1987), cytoskeletal arrangement (Pfeffer *et al*., 1980), and cellular morphology (Schuger *et al*., 1990). Although it is apparent that IFNs elicit these changes primarily through the transcriptional regulation of hundreds of genes (Boehm *et al*., 1997; Der *et al*., 1998), it remains unclear which induced or repressed proteins are responsible for which phenotypic changes.

The guanylate-binding proteins (GBPs) are a family of 67- to 69-kDa GTPases that are induced by IFN-α/β and IFN-γ, as well as tumor necrosis factor (TNF)-α and interleukin (IL)-1 (Vestal, 2005; Olszewski *et al*., 2006; Degrandi *et al*., 2007). GBPs are unusual because their third region of nucleotide contact is different from that of other GTPases (Cheng *et al*., 1991; Praefcke *et al*., 1999). Consequently, GBPs hydrolyze guanosine triphosphate (GTP) to both guanosine diphosphate (GDP) and guanosine monophosphate (GMP) (Schwemmle and Staeheli, 1994; Neun *et al*., 1996). Considerable structural and biochemical information has been obtained for one of the human (h) family members, hGBP-1. In addition to solving the crystal structures of full-length hGBP-1 without nucleotide (Prakash *et al*., 2000a) and with

nonhydrolyzable GTP analogue (Prakash *et al*., 2000b), and the amino-terminal globular GTP binding domain alone (Ghosh *et al*., 2006), much is known about the biochemical properties of hGBP-1 in solution and the contribution of individual amino acids to those properties (Praefcke *et al*., 1999, 2004; Kunzelman *et al*., 2005; Abdullah *et al*., 2009). Although some GBPs are robustly induced by IFN-γ treatment (Boehm *et al*., 1998), information on the role of GBPs in IFN responses is only recently emerging and is still incomplete.

hGBP-1 inhibits growth factor-induced proliferation of endothelial cells (Guenzi *et al*., 2001) and the expression of matrix metalloproteinase (MMP)-1 (Guenzi *et al*., 2003). This inhibition of MMP-1 results in decreased endothelial cell invasion and capillary tube formation (Guenzi *et al*., 2003). In addition, hGBP-1 protects tumor cells from killing by the chemotherapeutic drug paclitaxel (Duan *et al*., 2005). It is also suggested to inhibit apoptosis of endothelial cells upon growth factor withdrawal (Guenzi *et al*., 2001) and intestinal epithelial cells in a model of inflammatory bowel disease (Schnoor *et al*., 2009). hGBP-1 has modest antiviral activity against encephelomyocarditis virus (EMCV) and vesicular stomatitis virus (VSV) (Anderson *et al*., 1999) and inhibits replication of the hepatitis C virus replicon (Itsui *et al*., 2006). In addition, antimicrobial activity is suggested by the discovery of secreted hGBP-1 in cerebral spinal fluid of patients with bacterial meningitis (Naschberger *et al*., 2006). Recently, forced expression of hGBP-1 in human umbilical vein endothelial cells (HUVECs) was shown to inhibit their spreading on fibronectin (FN) (Weinlander *et al*., 2008).

New information is also available on the properties of some murine GBPs. mGBP-2, the putative murine orthologue of hGBP-1, also alters cell proliferation (Gorbacheva *et al*., 2002), modestly inhibits VSV and EMCV (Carter *et al*., 2005), and protects cells from killing by paclitaxel (Balasubramanian *et al*., 2006). Murine GBPs are also suggested to have antimicrobial properties. Murine GBP-5 promotes pyroptosis in human macrophage-like RAW 264.7 cells upon *Salmonella* infection, which might also be antimicrobial (Rupper and Cardelli, 2008). Mice infected with *Listeria monocytogenes* up-regulate expression of several of the murine GBPs, particularly mGBP-1, mGBP-2, and mGBP-7 (Degrandi *et al*., 2007). When mGBP expression was measured in murine lung and spleen after *Toxoplasma gondii* infection, the levels of all GBPs were increased by day 5 of infection (Degrandi *et al*., 2007). When RAW 264.7 macrophages were transfected with DsRed fusion constructs for some mGBPs (mGBP-6, mGBP-7, and mGBP-9) and treated with IFN-γ before infection with *T. gondii* type II strain ME49, mGBP-1, -2, -3, -6, -7, and -9 all relocalized to the parasitophorous vacuole within 30 min (Degrandi *et al*., 2007). IFN-γ treatment was required for this localization, suggesting that one or more other IFN-γ–induced proteins are required for this localization. These data suggest that at least some of the mGBPs may be involved in modulating *T. gondii* infection (Degrandi *et al*., 2007).

When mGBP-2 was cloned, NIH 3T3 fibroblasts were used to analyze its functional properties because they respond well to both IFN-α/β and IFN-γ. Early in the characterization of mGBP-2–expressing NIH 3T3 cells, it was noticed that the cells took longer to adhere and spread when transferred. The data from this study provide the first direct evidence that IFN-γ alters both fibroblast cell spreading on FN and after platelet-derived growth factor (PDGF) treatment. The study also identifies mGBP-2 as the IFN-regulated protein responsible for this inhibition of cell spreading and shows that the inhibition of cell spreading is not limited to fibroblasts but also occurs in B16 melanoma cells. mGBP-2 inhibits cell spreading by inhibiting signals from integrins or PDGF receptor that should activate Rac to promote cytoskeletal rearrangement. The inhibition of cell spreading by mGBP-2 is accompanied by the inhibition of phosphatidylinositol 3-kinase (PI3-K) activation.

MATERIALS AND METHODS

Antibodies and Matrix Proteins

Rabbit polyclonal antiserum against mGBP-2 was described previously (Vestal *et al*., 2000). Anti-FLAG monoclonal antibody M2 and rabbit anti-actin (A2066) were purchased from Sigma-Aldrich (St. Louis, MO). Anti-myc (9E10) antibody was purchased from Santa Cruz Biotechnology (Santa Cruz, CA). Purified human fibronectin and mouse laminin were purchased from Roche Molecular Biochemicals (Indianapolis, IN). Mouse type IV collagen was purchased from Invitrogen (Carlsbad, CA). Mouse anti-Rac was purchased from BD Biosciences Transduction Laboratories (Lexington, KY). Murine recombinant (r)IFN-γ was purchased from Calbiochem (San Diego, CA) or PBL InterferonSource (Piscataway, NJ), and PDGF was purchased from Calbiochem.

Expression Constructs

The plasmids pRK5, pRK5 myc-Rac1(G12V), pRK5 myc-Cdc42(G12V), and pRK5 myc-RhoA(G14V) were a gift from Dr. Amy Wilson-Delfosse (Case Western Reserve University, Cleveland, OH). The plasmid for the p21-activated kinase (PAK) binding domain (PBD) of PAK1 as a glutathione transferase (GST)-fusion protein was obtained from Richard Cerione via Lawrence Quilliam (Indiana University-Purdue University Indianapolis, Indianapolis, IN). The generation of the plasmid c-myc-pcDNA3.1hygro(−) was described previously (Gorbacheva *et al*., 2002). The plasmid c-myc-mGBP-2-pcDNA3.1 was generated by excising mGBP-2 from FLAG-mGBP-2-pCMV2(NH) (Vestal *et al*., 1998) by using Not1/Kpn1 and ligation into Not1/Kpn1 cut c-myc-pcDNA3.1hygro(−). mGBP-1 was cloned using reverse transcription-polymerase chain reaction (RT-PCR) from RAW 264.7 cells treated with 500 U/ml IFN-γ for 18 h using 5′-ATATGCGGCCGCGCCTCAGAGATCCACATGTCG-3′ and 5′-GGTACCTTAAAGTATGGTGCATGATCGAGGTGGAGGCATGTTC-3′ as forward and reverse primers, respectively.

Cells and Adhesion Assays

NIH 3T3, RAW 264.7, WEHI-3, and B16 cells were obtained from American Type Culture Collection and are maintained in DMEM (Mediatech, Herndon, VA) containing 10% fetal bovine serum (BioSource International, Camarillo, CA), 2 mM glutamine (Mediatech), and 50 U/ml penicillin/streptomycin (Mediatech). The FLAG epitope-tagged eukaryotic expression vectors containing either wild type or S52N mGBP-2 were generated and used to make stable cell lines in NIH 3T3 cells as described previously (Vestal *et al*., 2000; Gorbacheva *et al*., 2002). Characterization of the expression levels and growth characteristics of these clones were described previously (Gorbacheva *et al*., 2002). To generate B16 cells that stably express mGBP-2, cells were transfected with either pcDNA 3.1 myc or pcDNA 3.1 myc mGBP-2 using ExpressFect (Denville Scientific, Denville, NJ). Cells were selected in 300 μg/ml hygromycin, and pools of expressing and nonexpressing cells were analyzed for mGBP-2 expression and cell spreading as described below. Adhesion assays were performed using two different methods. First, cells were gently suspended in 0.05% trypsin/0.53 mM EDTA (Invitrogen) followed by DMEM containing 200 μg/ml soybean trypsin inhibitor (Sigma-Aldrich). After pelleting, cells were resuspended in DMEM containing 1% bovine serum albumin (BSA) and plated at 6×10^5 cells/well in 24-well dishes. The assays were also performed in 96-well format by plating 1×10^5 cells/well. After 20 min, the cells were washed and fixed with 2.5% glutaraldehyde. The attached cells were stained with 0.5% crystal violet, washed, and extracted with 1% SDS. The results were quantified by absorbance at 538 nm. The second method involved labeling cells with 4 μM calcein calcein AM (AM) (Invitrogen) per manufacturer's instructions before plating cells. After removal of nonadherent cells, adherent cells were measured by absorbance at 530 nm. Dishes were also coated with purified human fibronectin per manufacturer's instructions before adhesion assays. After coating, wells were blocked with 1% BSA in phosphate-buffered saline (PBS) overnight at 4°C.

Spreading Assays and Quantification of Cell Surface Areas

Coverslips (12-mm circles) in 24-well dishes were coated with FN (10 μg/ml). Cells were gently suspended by treatment with 0.05% trypsin/0.53 mM EDTA (Invitrogen); trypsin inhibitor (Sigma-Aldrich) was added to 0.2 mg/ml; and then cells were washed twice in DMEM, diluted in DMEM, and allowed to recover in suspension for 30 min at 37°C. Cells ($2.5–5 \times 10^4$) were plated per coverslip and allowed to adhere for 20, 40, or 60 min. Unattached cells were removed by gentle washing, and attached cells were fixed for 45

min with 4% paraformaldehyde. Coverslips were mounted in 50% VECTASHIELD (Vector Laboratories, Burlingame, CA) in PBS. Images were collected using either a MicroMax-1300Y camera (Roper Scientific, San Diego, CA) on a DMR upright microscope or a DM IRB HC inverted microscope (both Leica Microsyste, Deerfield, IL) with a cooled Retiga EX monochrome digital camera and analyzed with Image-Pro Plus software. For surface area determination, calibration was performed with a stage micrometer to provide the information of pixels per micrometer for the appropriate objective. To measure the surface areas, the perimeter of each cell was carefully outlined and its surface area was calculated by Image-Pro Plus, using the pixels per micrometer provided. The control transfectants (empty vector) varied in surface area from 200 μm^2 to >3000 μm^2. Surface areas of 100 cells per type were measured, grouped into 14 increments of 200 μm^2, and expressed as the percentage of the adherent population of cells. The smallest increment (1) contained cells that had surface areas between 200 and 400 μm^2 and the largest increment (14) contained cells with areas between 2800 and 3000 μm^2. Cells were classified as "spread" or "unspread" based on measured size cutoffs of either 600 or 800 μm^2. The association between cell type or treatment and proportion of unspread cells was assessed using Cochran–Mantel–Haenszel (CMH) tests of association, stratified by experiment repetition. The significance level of each test was 0.05; a Bonferroni correction was applied to the significance for a particular comparison when three tests were done (i.e., $0.05/3 = 0.017$). Statistical analyses were performed using the SAS system (SAS Institute, Cary, NC). Once it had been decided that an unspread cell would be defined as one with a surface area of $\leq$600 μm^2, then the means, SDs, and p values were calculated using Excel (Microsoft, Redmond, WA). Although results from a single transfection and isolation are shown, they were confirmed using transfectants from a second transfection process and isolation.

Control transfectants and mGBP-2–expressing cells (5×10^5/10-cm dish) were transfected with 6 μg of myc-tagged Rac1(G12V), RhoA(G14V), Cdc42(G12V), or pRK5 using ExpressFect (Denville Scientific), according to manufacturer's instructions. Twenty-four hours later, cells were processed for spreading as described above. After spreading on FN-coated coverslips for 25 min, cells were fixed and processed for two-color indirect immunofluorescence as described below using anti-Myc and anti-mGBP-2 as primary antibodies. Surface areas of stained cells were quantified by Image-Probsoftware, as described above.

Small Interfering RNA (siRNA) Transfections and Analyses

NIH 3T3 cells (3.25×10^4) were plated into individual wells of a 24-well dish and cotransfected with 50 nM RISC-FREE transfection control and either 50 nM mGBP-2 SMART Pool siRNA (a pool of 5 siRNAs: 5′-GCUGUGUGGUGAAUUUGUAUU-3′, 5′-GUUGAAACACUUCUACAGAUU-3′, 5′-AGACGAUUCCGCUAACUUUUU-3′, 5′-CAAAACAAAUCGUCUGGGAUU-3′), 50 nM cyclophilin B siRNA (5′-GGAAAGACUGUUCCAAAA-3′), or 50 nM nontarget siRNA (5′-UAGCGACUAAACACAUCAA-3′) using Dharmafect #1. All siRNAs were from Dharmacon RNA Technologies (Lafayette, CO). Thirty hours after transfection, the cells were treated with IFN-γ (500 U/ml) for 18 h. For Western blot analysis, cells from six wells of the 24-well dish were lysed, combined, and 20 μg of cell lysates were analyzed as described by Western blots. For spreading assays, multiple wells were transfected and treated. The cells were suspended, and 1.5×10^5 cells of each type were plated onto FN-coated coverslips for 40 min. The surface areas of cells containing RISC-FREE reagent (red perinuclear staining) were determined.

Actin Staining

Cells were plated onto coverslips in complete media overnight and then incubated in serum-free media for 2 h. After treatment with PDGF (10 ng/ml) for 0, 5, or 10 min, cells were washed, and actin filaments were labeled by fixing with 4% paraformaldehyde in PHEM buffer [60 mM piperazine-*N*,*N*′-bis(2-ethanesulfonic acid), 25 mM HEPES, 5 mM EGTA, 1 mM $MgCl_2$, 3% sucrose, and 0.1% Triton-X 100] containing 10 μl of Alexa 594-conjugated phalloidin (Invitrogen) per 200 μl for 20 min at 37°C. Cells were washed three times with PBS and mounted in VECTASHIELD with 4,6-diamidino-2-phenylindole. Surface areas were determined as described above.

Indirect Immunofluorescence

Cells were processed for cell spreading as described above. Cells were fixed and stained as described previously (Vestal *et al*., 2000). The antibodies used were rabbit polyclonal anti-mGBP-2 (1851; 1:200), mouse anti-vinculin (1:100; Clone VIN-11-5; Sigma-Aldrich), Alexa 488-conjugated goat anti-mouse and anti-rabbit, and Alexa 594-conjugated goat anti-rabbit and anti-mouse (Invitrogen). Images were captured with a DM IRB HC inverted microscope (Leica Microsystems) with a cooled Retiga EX monochrome digital camera. Confocal images were collected using aTCS-SP spectophotometric laser scanning confocal microscope (Leica Microsystems). For staining with antiphosphotyrosine antibody (1:800; 4G10; Millipore, Billerica, MA), cells were processed for indirect immunofluorescence as described previously (Vestal *et al*., 2000), except for the inclusion of phosphatase inhibitors in the wash buffer. Images were all collected keeping the gain, offset, and zoom constant. No adjustments were made in image intensity when the figures were prepared.

RT-PCR for Murine Integrin α_4

To examine cells for the expression of integrin α_4, RNA was isolated from cells using RNeasy mini kit (QIAGEN, Valencia, CA) per the manufacturer's instructions. cDNA was generated using 1.5 μg of total RNA using the SuperScript First Strand Synthesis kit (Invitrogen) and the random hexamers provided. PCR amplification was performed using 1.5 μg of cDNA and two different PCR primer pairs for α_4. The two different primer pairs were designed using the Pick Primers function at www.ncbi.nlm.nih.gov and the cDNA sequence at NM_010576. Each of these primer pairs was chosen to amplify a region of α_4 that spanned at least one intron, to control for possible DNA contamination of the samples and the primer pairs did not recognize any other sequences in the mouse database. The first primer pair has 5′-AGCTCCAGCTGGGTAGCCCC-3′ as forward and 5′-GGCTCCTCCCACGACTTCGGT-3′ as reverse primer. The second primer pair has 5′-TGGAAAGGGTCCTTGTCGGAAGTGA-3′ as forward and 5′-AGGCCTTGTCCTTAGCAACACTGC-3′ as reverse primer. The mouse glyceraldehyde-3-phosphate dehydrogenase primers used were 5′-CCAGGTTGTCTCCTGCGACT-3′ as forward and 5′-ATACCAGGAAATGAGCTTGACAAAGT-3′ as reverse.

Rac Activation Assays

To analyze Rac activation during cell spreading, control tranfectants and mGBP-2–expressing cells (5×10^6) were plated onto two 150-mm dishes and allowed to adhere overnight. After serum starving for 2 h, the cells were allowed to spread for 30 min in serum-free media onto two 100-mm fibronectin-coated (10-μg/ml) plates. Attached cells were lysed in 250 μl of lysis buffer per dish (50 mM Tris, pH 7.5, 10 mM $MgCl_2$, 1% IGEPAL CA-630 [Sigma-Aldrich], 150 mM NaCl, 1 mM sodium vanadate, 1 μl/ml protease inhibitor cocktail [Sigma-Aldrich], and 1 mM phenylmethylsulfonyl fluoride [PMSF]; Mira *et al*., 2000). Cell lysates were clarified by centrifugation at 13,000 $\times$ *g* for 3 min at 4°C. Cell lysates (500 μg) were added to 30 μg of PAK1 PBD/GST on beads in a final volume of 500 μl, and the samples were rotated at 4°C for 45 min. The resulting complexes were washed twice with 500 μl of lysis buffer and then twice with 500 μl of lysis buffer without IGEPAL. Complexes were dissociated and size fractionated on 10% PAGE gels. Total cell lysates (TCLs; 20 μg) were also included. Rac levels were determined by Western blot analysis and were quantified using 1D Scientific Imaging software (Eastman Kodak, Rochester, NY). The ratios of Rac from pull-downs and total cell lysates were determined and normalized to control cell samples for each blot.

To analyze Rac activation by PDGF, control transfectants and mGBP-2–expressing cells (5×10^6) were plated, allowed to adhere overnight, serum starved for 2 h, and treated with 10 ng/ml PDGF for 5 min. To analyze Rac activation by PDGF subsequent to IFN-γ treatment, cells were plated as described above, allowed to adhere for 4 h, and then serum starved in the presence or absence of IFN-γ (500 U/ml) for 18 h. Cells were lysed and processed for analysis of Rac activity as described above.

Phospho-Akt Assays

Control transfectants and mGBP-2–expressing NIH 3T3 cells were serum starved for 1 h and processed for cell spreading on FN. Adherent cells were lysed in 200 μl of cold radioimmunoprecipitation assay lysis buffer (50 mM Tris, pH 7.5, 150 mM NaCl, 1% NP-40, 0.5% sodium deoxycholate, 0.1% SDS, 1 μl/ml Protease inhibitor cocktail [Sigma-Aldrich], 1 mM PMSF, 25 mM sodium fluoride, 10 mM sodium vanadate, 100 μM sodium molybdate, and 50 mM sodium pyrophosphate) per 100-mm FN-coated dish on ice. Samples of the cells were also taken 1) after the 1-h serum starvation and 2) before plating but after the recovery in suspension. Lysates were clarified by centrifugation at 10,000 $\times$ *g* for 5 min at 4°C and analyzed by Western blot with anti-phospho-Akt antibodies as described below. The membranes were then stripped and immunodetected with antiserum against total Akt. Films were quantified using 1D Scientific Imaging software (Eastman Kodak) and the ratios of phospho-Akt and total Akt were determined.

Coimmunoprecipitations

Control, mGBP-2-, and/or S52N mGBP-2–expressing NIH 3T3 cells were plated at 5×10^6 cells per 150-mm dish and allowed to adhere overnight. Four 150-mm dishes were plated for each cell line. Cells were suspended and allowed to recover as described previously. The cells from all four 150-mm dishes were divided and plated onto two 150-mm FN-coated dishes for 35 min. Unattached cells were removed by gentle washing with Hanks' balanced salt solution containing 1 mM sodium vanadate. Adherent cells were lysed in 250 μl of Tris-buffered saline/Tween 20 lysis buffer (10 mM Tris, pH 7.4, 1 mM EDTA, 150 mM NaCl, 1.0% Triton X-100, 1 μl/ml Protease Inhibitor Cocktail [Sigma-Aldrich], 0.1 mM PMSF, 25 mM sodium fluoride, 10 mM sodium vanadate, 100 μM sodium molybdate, and 50 mM sodium pyrophosphate) per dish. Lysates were clarified by centrifugation at 10,000 $\times$ *g* for 5 min at 4°C. Cell lysates (500 μg) were added to 100 μl of FLAG M2 agarose (Sigma-Aldrich) or 5 μl of anti-PI3-K p110 antisera or FLAG M2 antisera in a

final volume of 500 μl of lysis buffer and rotated overnight at 4°C, followed by protein G-Sepharose for 1 h. The immune complexes were washed three times with 500 μl of lysis buffer and the immune complexes were dissociated in 5× Laemmli sample buffer by heating at 95°C for 4 min. Samples were size fractionated on SDS-PAGE gels and analyzed by Western blotting as described below. TCLs (20 μg) also were included.

PAGE Gels and Western Blots

PAGE and Western analysis of cell lysates were performed as described previously (Gorbacheva *et al*., 2002). Antibodies were used at 1:500 mouse anti-FLAG (M2), 1:1000 mouse anti-Rac (BD Biosciences Transduction Laboratories), 1:800 mouse anti-β_1 (BD Biosciences Transduction Laboratories), 1:5000 rabbit anti-α_5 (Millipore Bioscience Research Reagents, Temecula, CA), 1:800 rabbit anti-mGBP-2 (1851), 1:1500 rabbit anti-cyclophilin B (Ab16045; Santa Cruz Biotechnology), 1:500 mouse anti-IFN-γ–induced GTPase (IGTP; BD Biosciences Transduction Laboratories), 1:200 mouse anti-myc (Santa Cruz Biotechnology), 1:500 phospho-Akt (Cell Signaling Technology, Danvers, MA), 1:1000 anti-Akt (Cell Signaling Technology), 1:500 rabbit monoclonal anti-PI3-K p85α (04-403; Millipore; recognizes the C terminus), 1:200 rabbit polyclonal anti-PI3-K p110 (Sc-7189; Santa Cruz Biotechnology; reacts with p110α, -β, -γ, and -δ), and 1:300 for rabbit anti-actin (Sigma-Aldrich). Secondary antibodies used were horseradish peroxidase-conjugated goat anti-rabbit (1:10,000; Rockland Immunochemicals, Gilbertsville, PA), and anti-mouse (1:800; Invitrogen) and detected using enhanced chemiluminescence (GE Healthcare, Little Chalfont, Buckinghamshire, United Kingdom). Antibodies were removed using Restore Western blot stripping buffer (Pierce Chemical, Rockford, IL).

PI3-K Activity Assays

To analyze PK3-K activity during cell spreading on FN, control transfectants and mGBP-2–expressing cells were resuspended and processed for cell spreading on FN as described above. Twenty minutes after plating on FN, the nonadherent cells were removed by gentle washing and the adherent cells were lysed in 20 mM Tris-HCl, pH 7.4, 137 mM NaCl, 1 mM $CaCl_2$, 1 mM $MgCl_2$, 0.1 mM sodium vanadate, 1% NP-40, and 1 mM PMSF. Cell lysates (500 μg) were incubated with anti-p85 PI3-K antibody (06-195; Millipore) overnight at 4°C. Protein A-Sepharose was added for 1 h, and the immune complexes were washed and processed using a PI3-kinase activity enzyme-linked immunosorbent assay (ELISA) kit (Pico; Eschelon Biosciences, Logan, UT) and following the manufacturer's instructions. The level of phosphatidylinositol (3,4,5)-trisphosphate (PIP_3) generated by serum-starved control transfectants in each assay was set to 100%, and the values from all other samples were normalized to this.

RESULTS

The Interferon-Induced GTPase mGBP-2 Inhibits Cell Adhesion

The GBPs are an incompletely characterized family of large GTPases (Vestal, 2005; Olszewski *et al*., 2006; Degrandi *et al*., 2007). The murine family member mGBP-2 is not detected in NIH 3T3 cells before treatment with IFN-γ and only becomes detectable after 4 h of treatment (Vestal *et al*., 2000). Stable NIH 3T3 fibroblast cell lines expressing mGBP-2 have been established, and the expression levels of mGBP-2 in several of these cell lines are comparable with the level of mGBP-2 observed in untransfected cells after IFN-γ treatment for 24 h. This information has been published previously (Gorbacheva *et al*., 2002). During the characterization of these cell lines, we observed that cells expressing mGBP-2 did not attach as quickly to tissue culture dishes as the control transfectants (Figure 1). To explore the possibility that there was a defect in the ability of cells expressing mGBP-2 to adhere to FN, calcein AM was used to confirm that cells expressing mGBP-2 do not adhere as rapidly as control transfectants (empty vector) (Figure 1A). This observation was followed by experiments to determine whether there was also a defect in the ability of mGBP-2–expressing cells to spread on FN.

mGBP-2 Retards Cell Spreading on FN

Cell spreading is a complex process that follows cell attachment and involves the generation of new substrata adhesion sites, cytoskeletal reorganization, and lamellipodia formation (Small *et al*., 1999). mGBP-2–expressing NIH 3T3 cells were plated on FN-coated coverslips and allowed to attach/spread for 20 min (Supplemental Figure 1). Control transfectants (empty vector) exhibited surface areas ranging from 200 to 400 μm^2 (increment 1) to 2800–3000 μm^2 (increment 14). Comparison of the distribution of surface areas of the cells indicates that there are more mGBP-2–expressing cells in the smaller three size increments than control transfectants (Figure 1B). Only 16 ± 5% of the control cells had surface areas ≤600 μm^2 (increments 1 + 2), whereas 42 ± 10% of the mGBP-2–expressing cells failed to spread to surface areas >600 μm^2 (Figure 1C). Using a less stringent measure of an unspread cell (the first 3 increments, or ≤800 μm^2), there were still approximately twice as many mGBP-2–expressing cells that failed to spread compared with control cells (Figure 1C). Because the relative proportion of cells expressing mGBP-2 that remained poorly spread was the same with either the ≤600 or ≤800 μm^2 as a measurement of small, poorly spread cells, the more stringent cut-off of ≤600 μm^2 was chosen to represent unspread cells in subsequent experiments. Comparable results were obtained for other clones expressing mGBP-2 at similar levels (data not shown). mGBP-2 does not abolish the ability of NIH 3T3 cells to spread on FN, it just slows the process considerably. When the cells were plated on FN-coated coverslips and allowed to adhere for 24 or 48 h, both control and mGBP-2–expressing cells were able to spread to sizes >2400 μm^2 (Supplemental Figure 2, A and B).

S52N mGBP-2 Does Not Inhibit Cell Spreading on FN

NIH 3T3 cell lines that expressed S52N mGBP-2 at comparable levels to the mGBP-2–expressing cells evaluated in the previous experiments were generated and characterized previously (Gorbacheva *et al*., 2002). S52N mGBP-2 has a single amino acid substitution in the GTP binding domain of mGBP-2 that is analogous to the S17N substitution of Ras. Because this amino acid residue is involved in coordination of the magnesium necessary for GTP binding, when this mutation is generated it results in proteins with reduced affinity for GTP (Feig, 1999). The crystal structure of the highly homologous, putative human orthologue of mGBP-2, hGBP-1, showed that S52 of hGBP-1 is involved in coordination of the magnesium ion as observed for other GTPases (Prakash *et al*., 2000). In vitro studies of hGBP-1 suggest that it will be nucleotide free at cellular concentrations of guanine nucleotides (Praefcke *et al*., 2004). Although it has not been confirmed for mGBP-2, we expect that because of the high homology between hGBP-1 and mGBP-2 that S52N mGBP-2 will behave the same. NIH 3T3 cells expressing S52N mGBP-2 were examined for their ability to spread on FN (Figure 1, B and C, and Supplemental Figure 1). No significant difference was observed between the spreading of S52N mGBP-2–expressing cells and the control transfectants.

IFN-γ Treatment of NIH 3T3 Fibroblasts Retards Cell Spreading on FN

We examined the effect of IFN-γ treatment on NIH 3T3 cell spreading on FN. NIH 3T3 cells treated with IFN-γ for 8 and 18 h were allowed to spread on FN (Figure 1D and Supplemental Figure 1). By 8 h of IFN treatment, NIH 3T3 cells were retarded in their ability to spread (70 ± 10% had surface areas ≤600 μm^2 compared with 31 ± 12% for untreated cells) (Figure 1D). No additional reduction in spreading was observed after 18 h of IFN-γ treatment (70 ± 15% had areas ≤600 μm^2). IFN-γ treatment results in maximal mGBP-2 expression by 8 h, and expression remains high through 24 h (Gorbacheva *et al*., 2002).

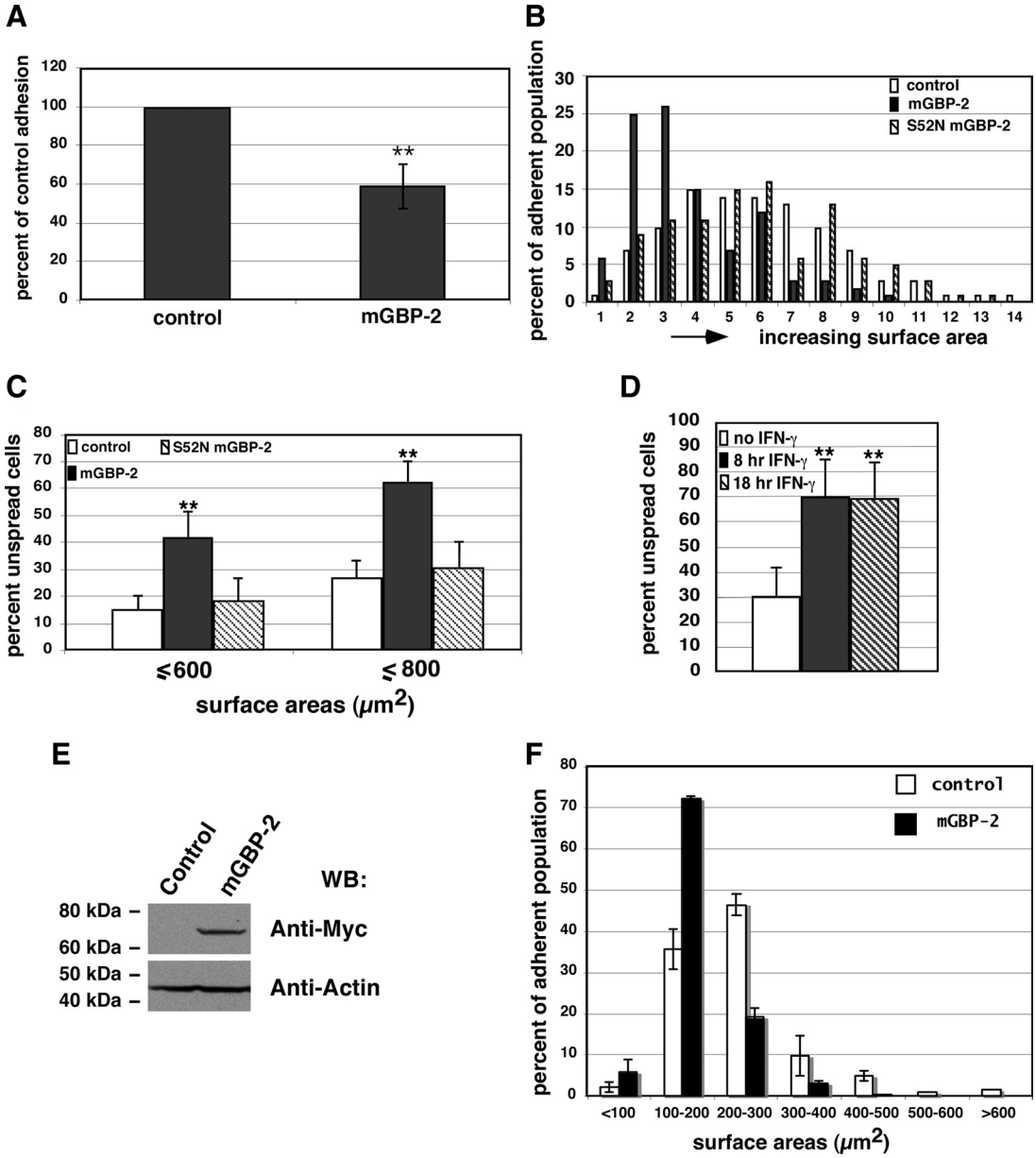

Figure 1. Either mGBP-2 expression or IFN-γ treatment retard NIH 3T3 cell spreading on FN. (A) Equal numbers of control transfectants and mGBP-2–expressing NIH 3T3 cells were labeled with 4 μM calcein AM, plated onto FN-coated dishes, and allowed to adhere for 20 min. After removal of nonadherent cells, relative numbers of adherent cells were measured by absorbance at 530 nm. The adhesion of the control cells was set to 100%, and the results expressed as the mean percentage of control adhesion ± SD (n = 4 experiments; *$p < 0.01$ compared with control). (B) Cells were plated onto coverslips coated with 10 μg/ml FN and allowed to adhere for 20 min before the nonadherent cells were removed and the adherent cells were fixed. The surface areas were measured as described in *Materials and Methods*. A representative breakdown of the surface areas from one experiment is shown. More mGBP-2–expressing cells failed to spread beyond 800 μm^2 (increments 1–3). (C) The retardation of cell spreading by mGBP-2 is represented graphically as the number of cells with surface areas ≤600 or ≤800 μm^2. The results represent the mean ± SD (n = 4). mGBP-2 expression was significantly associated with a greater proportion of unspread cells (**$p < 0.001$ compared with control cells [empty vector] for each size range) compared with control transfectants. (D) NIH 3T3 cells were treated with IFN-γ (300 U/ml) for 8 or 18 h and were allowed to adhere to FN-coated coverslips. Retardation of cell spreading by IFN-γ is represented graphically as the number of cells with surface areas ≤600 μm^2. The results represent the mean ± SD (n = 3). Treatment with IFN-γ for either 8 or 18 h was significantly associated with a larger proportion of unspread cells (**$p < 0.001$ compared with untreated cells). (E) Control transfectants (control) and mGBP-2–expressing B16 cells were lysed and mGBP-2 expression was examined using Western immunoblots with anti-Myc antisera. (F) Control and mGBP-2–expressing B16 cells were allowed to spread on FN as described previously. More mGBP-2–expressing cells had surface area of 200 μm2 or less than control cells (n = 2).

mGBP-2 Also Inhibits the Spreading of B16 Melanoma Cells on Fibronectin

To ask whether mGBP-2 can inhibit the spreading of other cells, murine B16 melanoma cells were generated that contained empty vector (control) or vector with myc epitope-tagged mGBP-2 (mGBP-2) (Figure 1E). The surface areas of the B16 cells after 20 min of spreading on FN is shown (Figure 1F). The B16 cells had spread to surface areas rang-

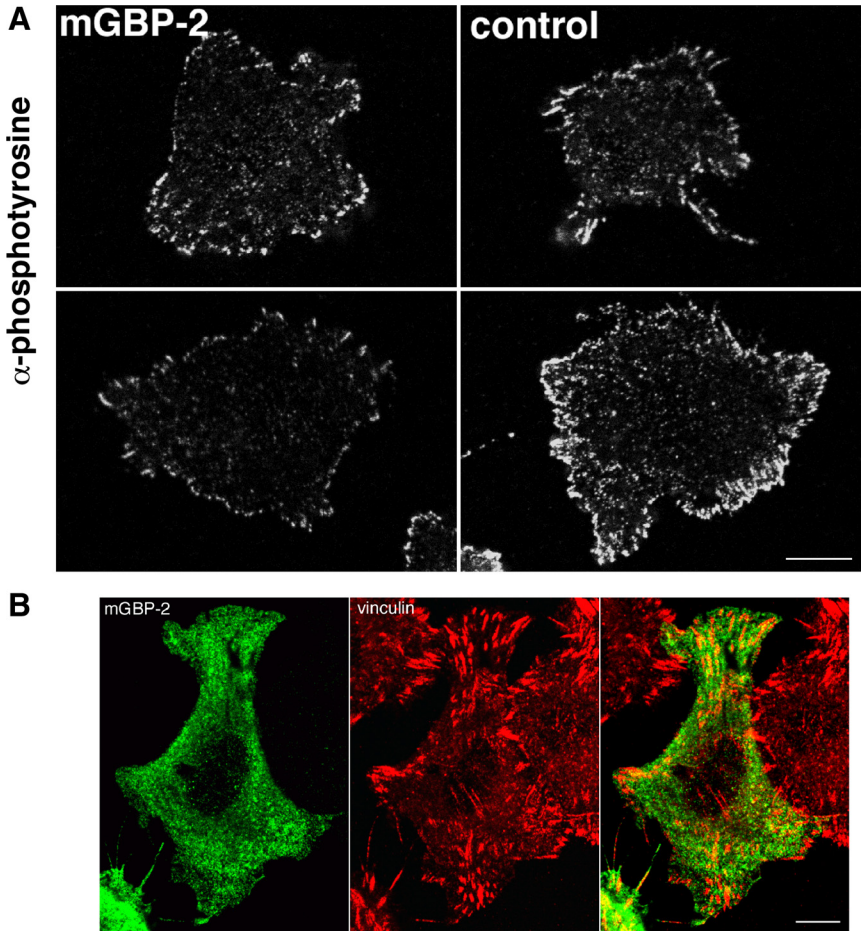

Figure 2. Examination of cell substrata attachments in mGBP-2–expressing NIH 3T3 cells. (A) Control and mGBP-2–expressing NIH 3T3 cells were allowed to spread on FN for 20 min and were stained for α-phosphotyrosine as described in *Materials and Methods*. Bar, 10 μm. (B) mGBP-2–expressing NIH 3T3 cells were allowed to spread on FN-coated coverslips for 30 min and stained for mGBP-2 and vinculin as described in *Materials and Methods*. Images were captured by confocal microscopy. Bar, 5 μm.

ing from <100 μm^2 to just >600 μm^2 in 20 min. However, just over twice as many of the B16 cells expressing mGBP-2 still had surface areas in the smallest two increments (<100–200 μm^2) after 20 min on FN compared with the control transfects. When B16 control and mGBP-2–expressing cells are allowed to spread on FN for 24 h (Supplemental Figure 2C), the number of mGBP-2–expressing B16 cells in the smaller increments is not more than observed for the control transfectants. From this, we conclude that mGBP-2 inhibits cell spreading in the B16 melanoma cells.

Examination of Cell–Substrata Attachment Sites in Cells Expressing mGBP-2

To further characterize the differences in control transfectant and mGBP-2–expressing NIH 3T3 cells during cell spreading, cells were allowed to spread for 20 min on FN and were examined by staining for phosphotyrosine (Figure 2A). Examination of phosphotyrosine staining at the basal surface of spreading cells allows visualization of cell–substrata contact sites where active signaling events are occurring. The images presented are from the basal surface of the cells and have been captured under the same conditions. Although there was significant heterogeneity in the phosphotyrosine staining even within the control or mGBP-2–expressing cells, when cells of comparable sizes were compared the staining at the basal surface tended to be less bright and the foci of staining somewhat smaller in the mGBP-2–expressing NIH 3T3 cells. Whether mGBP-2 was concentrated at sites of focal adhesions was examined by double-label indirect immunofluorescence for mGBP-2 and vinculin in cells spreading on FN (Figure 2B). mGBP-2 has a punctate distribution throughout the cytoplasm and is not appreciably colocalized with vinculin, suggesting that little, if any, mGBP-2 is found in focal adhesions.

mGBP-2–specific siRNAs Rescue IFN-γ-mediated Inhibition of Cell Spreading

To determine whether mGBP-2 is required for IFN-γ-mediated inhibition of cell spreading, mGBP-2–specific siRNAs were used to knockdown the expression of mGBP-2 in IFN-γ–treated NIH 3T3 cells (Figure 3). NIH 3T3 cells were cotransfected with RISC-FREE transfection control and mGBP-2 siRNAs, cyclophilin B siRNA, or nontarget siRNA. After 30 h, the cells were treated with IFN-γ, and the specificity of the knockdowns were evaluated (Figure 3A). As expected, in the absence of IFN-γ no mGBP-2 is detected. In the presence of the mGBP-2 siRNAs, the level of mGBP-2 after IFN-γ treatment is reduced by >80% (Figure 3A). Nontarget and cyclophilin B siRNAs have no effect on mGBP-2 expression. The mGBP-2 siRNAs have no effect on the expression of another IFN-γ–induced GTPase, Irgm3 (formerly IGTP) (Bekpen *et al.*, 2005), or on the level of cyclophilin B. To determine whether IFN-γ treatment could still inhibit cell spreading in the absence of mGBP-2, NIH 3T3 cells were transfected with RISC-FREE transfection control and either nontarget siRNA or mGBP-2–specific siRNAs; treated with IFN-γ; and analyzed for cell spreading (Figure 3B). The knockdown of mGBP-2 completely rescued IFN-γ–induced

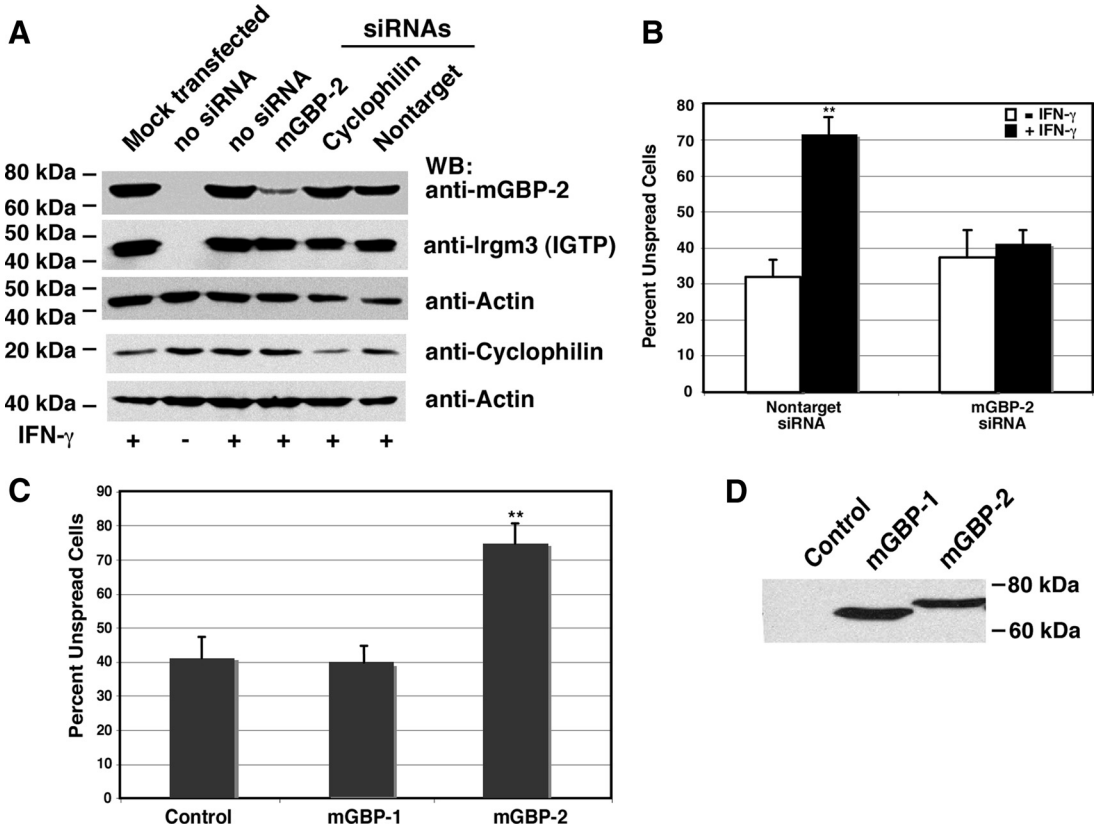

Figure 3. Knockdown of mGBP-2 expression in IFN-γ–treated cells restores cell spreading. NIH 3T3 cells were cotransfected with 50 nM RISC-FREE transfection control and 50 nM of either mGBP-2 Smart Pool siRNAs, cyclophilin B siRNA, or nontarget siRNA. After 30 h, cells were treated with 500 U/ml rmIFN-γ for 18 h. (A) Total cell lysates (20 μg) were separated by SDS-PAGE on 8 or 12% gels, followed by Western analysis. A representative blot is shown (n = 2). (B) siRNA-transfected and IFN-γ–treated NIH 3T3 cells (3.2×10^5) were allowed to adhere to FN-coated coverslips for 40 min. The surface areas of cells containing RISC-FREE transfection control were measured and expressed as percentage of unspread cells. Results are the means ± SD (**$p < 0.01$ compared with untreated cells receiving nontarget siRNA; n = 3). (C) NIH 3T3 cells were transfected with pCMV-EGFP and either control vector, myc-mGBP-2, or myc-mGBP-1 (ratio 1:3). After 24 h, EGFP-expressing cells were evaluated for spreading on FN. Results are expressed as mean percentage of unspread cells ± SD (*$p < 0.001$ compared with control cells receiving empty vector; n = 3). (D) Cell lysates (20 μg) from cells transfected in C were separated on 8% PAGE gels and analyzed by Western blot with anti-myc antisera. A representative blot is shown (n = 2).

inhibition of cell spreading (Figure 3B). Although IFN-γ induces the expression of all of the murine GBPs (Degrandi *et al.*, 2007), mGBP-1 is the most closely related murine GBP to mGBP-2, with ~80% amino acid identity (Olszewski *et al.*, 2006). All other murine GBPs are significantly different from mGBP-2 (identities in the 50% range). No good commercial antibodies against mGBP-1 are available to determine whether the siRNAs against mGBP-2 have any effect on the expression of mGBP-1. To rule out a contribution of mGBP-1 to IFN-γ–initiated inhibition of cell spreading, cells were transiently transfected with mGBP-1 or mGBP-2 and their relative abilities to inhibit spreading on FN were evaluated. mGBP-1 was unable to inhibit cell spreading (Figure 3C). Therefore, we conclude that mGBP-2 is the major contributor to IFN-γ–mediated inhibition of cell spreading.

Neither IFN-γ Treatment nor mGBP-2 Expression Reduced the Levels of the FN Receptor $\alpha_5\beta_1$ or Promoted the Expression of Integrin α_4

IFN-γ treatment of cells can result in the transcriptional regulation of hundreds of genes, including a number of integrins (Boehm *et al.*, 1997; Der *et al.*, 1998). Adhesion of NIH 3T3 cells to FN is mediated primarily by the integrin heterodimer $\alpha_5\beta_1$. IFN-γ treatment for as long as 48 h did not alter the amount of α_5 or β_1 expressed by NIH 3T3 cells (Supplemental Figure 3, A and B). In addition, IFN-γ treatment for up to 48 h did not alter the steady-state expression of the linker proteins talin, vinculin, paxillin, or α-actinin (data not shown). Similar to treatment with IFN-γ, mGBP-2 expression did not reduce the steady-state levels of α_5 or β_1 (Supplemental Figure 3, B and C) or the linker proteins talin, vinculin, paxillin, or α-actinin (data not shown). In fact, they have slightly increased levels of surface α_5 or β_1.

To determine whether increasing the FN concentration could restore cell spreading, control and mGBP-2–expressing cells were allowed to spread on concentrations of FN ranging from 2 to 20 μg/ml (Supplemental Figure 2D). Increasing the concentration of FN beyond 10 μg/ml did not increase cell spreading, suggesting that mGBP-2 does not inhibit cell spreading by reducing integrin affinity.

While preparing this manuscript, it was reported that the putative human orthologue of mGBP-2, hGBP-1, inhibits HUVEC cell spreading and that this phenotypic change is correlated with the up-regulation of integrin α_4 (Weinlander *et al.*, 2008). Examination of NIH 3T3 cells showed mGBP-2 expression did not induce the expression of integrin α_4 (Supplemental Figure 3D).

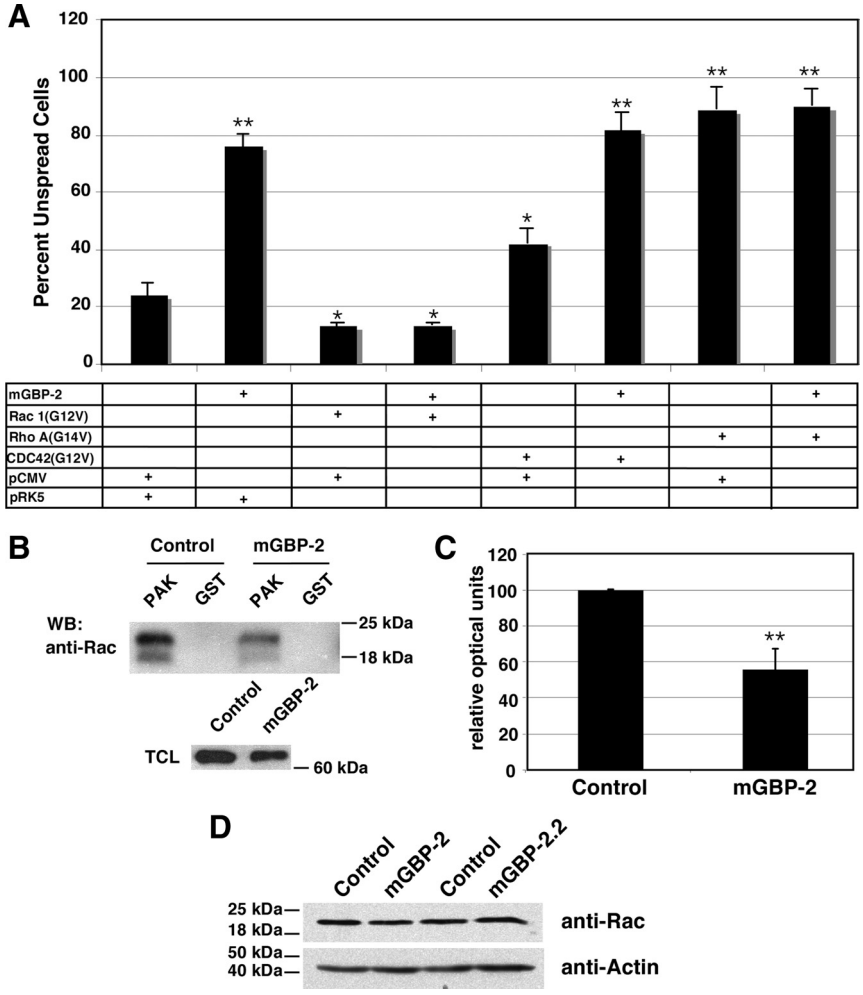

Figure 4. mGBP-2 inhibits Rac activation during cell spreading on FN. (A) NIH 3T3 cells were transfected with the plasmids listed below the graph. After 24 h, the cells were processed for cell spreading on FN as described above. After 30 min of attachment, cells were fixed and processed by two-color indirect immunofluorescence for the Myc-epitope tagged Rho family members (anti-Myc) and mGBP-2 (polyclonal anti-mGBP-2), as described in Materials and Methods. The surface areas of cells expressing the Rho family member alone or in combination with mGBP-2 were measured and the results are expressed as mean percentage of unspread cells ($\leq$600 μm^2) $\pm$ SD (n = 3; *$p < 0.05$ or **$p < 0.01$ compared with vector control). (B) Control transfectants (empty vector) and mGBP-2–expressing NIH 3T3 cells were allowed to spread on FN-coated dishes (10 μg/ml) for 30 min, harvested, and analyzed for relative levels of active Rac. The Rac-PAK PBD/GST complexes were denatured, size fractionated by PAGE, and analyzed by Western blot for Rac. TCLs from control transfectants and mGBP-2–expressing cells were used for normalization in the quantification of active Rac. A representative blot of four experiments is shown. (C) Western blots from PBD pull-downs were quantified, and the results for levels of active Rac were normalized to total cellular Rac and then set to 100% for control cells (**$p < 0.01$ compared with control transfectants; n = 4). (D) To confirm that mGBP-2 expression did not alter the level of Rac, TCLs (20 μg) from two different control transfectant and mGBP-2–expressing cell lines were analyzed for Rac by Western analysis.

The initial observation that mGBP-2–expressing cells took longer to stably adhere to uncoated culture dishes suggested that the inhibition of spreading might not be FN dependent. The spreading of mGBP-2–expressing cells was examined on both collagen IV and laminin. Cell spreading on collagen IV and laminin took more time than on FN (40 vs. 20 min), but the same trend toward slower spreading by mGBP-2–expressing cells was observed. On collagen IV, fewer control transfectants remained unspread ($\leq$600 μm^2; 50.5 $\pm$ 10%) compared with mGBP-2–expressing cells (68 $\pm$ 2%; n = 2) (data not shown). On laminin, again fewer control cells (26.6 $\pm$ 4%) remained unspread compared with mGBP-2–expressing cells (59.3 $\pm$ 9%; n = 2) (data not shown). mGBP-2 inhibition of cell spreading is not dependent on a particular (Zhang *et al.*, 2006) integrin; therefore, it might be through the inhibition of intracellular signals regulating the actin cytoskeleton and be common to many integrins.

mGBP-2 Inhibits Rac Activation Initiated by Cell Adhesion/Spreading

Members of the Rho family of small GTPases are master regulators of the actin cytoskeleton, mediating cell spreading (Hall, 1998; Price *et al.*, 1998; Ridley, 2000). To determine whether Rac1, Cdc42, or RhoA are downstream of mGBP-2–mediated inhibition, their ability to rescue cell spreading was examined. Control transfectants (pCMV) or mGBP-2–expressing NIH 3T3 cells were transfected with either Rac1(G12V), RhoA(G14V), Cdc42(G12V), or empty pRK5 and spreading on FN was analyzed (Figure 4A). After transfection with empty pRK5, control mGBP-2–expressing cells were still significantly inhibited in their ability to spread on FN compared with control transfectants (75.8 $\pm$ 4.2 vs. 23.97 $\pm$ 4.4%). As shown in other cells, expression of Rac1(G12V) in control transfectants promotes cell spreading (13.1 $\pm$ 1.5 vs. 23.97 $\pm$ 4.4% unspread cells) (Zhang *et al.*, 2006). As expected, both RhoA(G14V) (88.9% unspread cells) and Cdc42(G12V) (42.0 $\pm$ 5.4%) inhibited cell spreading. However, only Rac1(G12V) was capable of restoring cell spreading in the presence of mGBP-2 (13.4 $\pm$ 0.9% unspread cells) (Figure 4A). These data suggest that mGBP-2 is upstream of Rac1. If this is correct, cell spreading in the presence of mGBP-2 should result in lower levels of activated Rac. Consistent with this prediction, less activated Rac is detected in mGBP-2–expressing cells as they spread on FN (Figure 4, B and C). Because the cells were serum-starved to quiet signaling before adhesion/spreading, the levels of active Rac was below the level of detection in cells before suspension and restimulation by plating onto FN. Although there is sometimes some variability in the level of Rac observed in the TCLs from the spreading cells, these differences are compensated for when the quantifications for active Rac are normalized for differences in Rac in the TCLs. mGBP-2 does not itself alter the level of Rac in NIH 3T3 cells (Figure 4D).

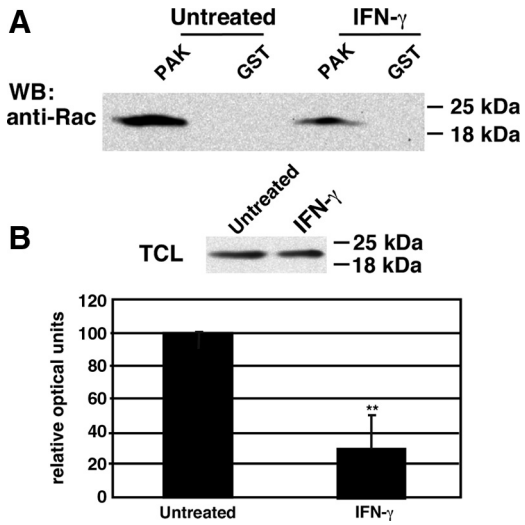

Figure 5. IFN-γ treatment results in inhibition of Rac activation during cell spreading on FN. (A) NIH 3T3 cells were treated with IFN-γ (500 U/ml) for 24 h and then were allowed to spread on FN-coated dishes (10 μg/ml) for 30 min. Next, they were harvested and analyzed for the levels of active Rac. The Rac-PAK PBD/GST complexes were denatured, size fractionated by PAGE, and analyzed by Western blot for Rac. TCLs were used to confirm that IFN-γ treatment did not change the expression levels of Rac. A representative blot of three experiments is shown. (B) Western blots from PBD pull-downs were quantified, and the results for levels of active Rac were normalized to total cellular Rac and then set to 100% for control (untreated) cells (**$p < 0.01$ compared with untreated cells; $n = 3$).

IFN-γ Treatment Also Inhibits Rac Activation during Cell Spreading

Consistent with Rac inhibition being critical to the inhibition of spreading by IFN, IFN-γ treatment also inhibits Rac activation during cell spreading (Figure 5, A and B).

mGBP-2 Inhibits Cell Spreading Initiated by PDGF Treatment

Integrin engagement is not the only physiological stimulus for cell spreading. PDGF can also induce flattening and spreading in several cell types, a process that is Rac dependent (Symes and Mercola, 1996; James *et al*., 2004; Petroll *et al*., 2008; Abramovici *et al*., 2009). To ask whether mGBP-2 could inhibit the spreading of cells induced by PDGF treatment, control transfectants and mGBP-2–expressing cells on uncoated coverslips were serum starved for 2 h and treated with PDGF for 5 or 10 min and stained with phalloidin (Figure 6D). The surface areas were measured and the size distributions of untreated control transfectants and mGBP-2–expressing cells are shown in Figure 6A. Before treatment with PDGF, the cells seem to shrink in surface area compared with cells in complete media (Figure 6A vs. Supplemental Figure 2), but there are no striking differences in the surface areas of control transfectants versus mGBP-2–expressing cells. After 5 min of PDGF treatment the control cells have increased in size, whereas the mGBP-2–expressing cells remained comparable in size to before treatment (Figure 6, B and D). After 10 min of PDGF treatment, the differences between the surface areas of the PDGF-treated control and mGBP-2–expressing cells persists (Figure 6, C and D). Together, these data demonstrate that PDGF treatment of NIH 3T3 cells does increase their surface areas and that the expression of mGBP-2 inhibits this spreading.

mGBP-2 and IFN-γ Treatment Inhibits Rac Activation by PDGF

Rac can be activated by a variety of stimuli, including integrin engagement, growth factors, cadherins, immunoglobulin superfamily receptors, and G protein-coupled receptors (Schwartz, 2004). Rac activation by PDGF was examined in the presence and absence of mGBP-2 (Figure 7A). As expected, PDGF treatment of control transfectants resulted in Rac activation (Figure 7A). In the presence of mGBP-2, this activation was attenuated by ~50% (Figure 7B). Consistent with this, IFN-γ treatment of untransfected cells also resulted in inhibition of Rac activation upon PDGF treatment (Figure 7, C and D). Together, these data show that sustained IFN-γ treatment inhibits Rac activation by both integrin engagement and PDGF treatment, as a consequence of mGBP-2 induction. PDGF treatment itself does not induce the expression of mGBP-2 and does not alter the level of mGBP-2 induced by IFN-γ (Figure 7E).

mGBP-2 Inhibits Akt Activation in Spreading Cells

Having demonstrated that Rac is inhibited by mGBP-2 subsequent to plating on FN or PDGF treatment, we wanted to know where in the pathway(s) from these two stimuli mGBP-2 acts. Operating on the hypothesis that the protein(s) directly inhibited by mGBP-2 would need to come into contact with mGBP-2, immunoprecipitations were used to determine whether mGBP-2 interacts directly with Rac during cell spreading (data not shown). No direct interaction between the two proteins was detected, suggesting to us that mGBP-2 probably does not act directly on Rac. Forced overexpression of the Rac guanine exchange factor Tiam-1 was able to rescue cell spreading in mGBP-2–expressing cells, but no direct interaction between mGBP-2 and Tiam-1 was detected (data not shown). This suggested that the point of inhibition by mGBP-2 was more proximal to integrin or PDGF receptor.

PI3-K is a major contributor to the activation of Rac upon either integrin engagement or PDGF treatment (Bokoch *et al*., 1996; Symes and Mercola, 1996; Welch *et al*., 2003). For this reason, PI3-K is a critical component of the signaling cascade(s) involved in lamellipodia formation and cell spreading (Wennstrom *et al*., 1994; Berrier *et al*., 2000; Hermanto *et al*., 2002; Welch *et al*., 2003; Qian *et al*., 2005; Lasunskaia *et al*., 2006). PI3-K activation was analyzed indirectly by monitoring changes in the levels of active Akt (phospho-Akt) during cell spreading in the presence or absence of mGBP-2 (Figure 8, A and B). pAkt levels were reduced significantly in the presence of mGBP-2, suggesting that mGBP-2 may inhibit PI3-K activity.

mGBP-2 Is Found in a Protein Complex Containing the p110 Catalytic Subunit of PI3-K

To determine whether PI3-K is the point of interaction with mGBP-2, we asked whether mGBP-2 forms a protein complex with one or more of the subunits of PI3-K. To answer this, cell lysates from control or mGBP-2–expressing cells spreading on FN were immunoprecipitated with anti-FLAG antibody to isolate mGBP-2. Western blot analyses showed that the p110 subunit of PI3-K is part of a protein complex containing mGBP-2 (Figure 8C). We confirmed this interaction by immunoprecipitation with anti-p110 antisera (Figure 8D). In cell lysates immunoprecipitated with anti-FLAG to isolated mGBP-2 and subsequently immunodetected with antisera for p85, the level of p85 in the immune complexes generated in the presence of mGBP-2 was not above background (Figure 8C). We conclude from this that little, if any, p85 is in the same protein complex as mGBP-2 and p110.

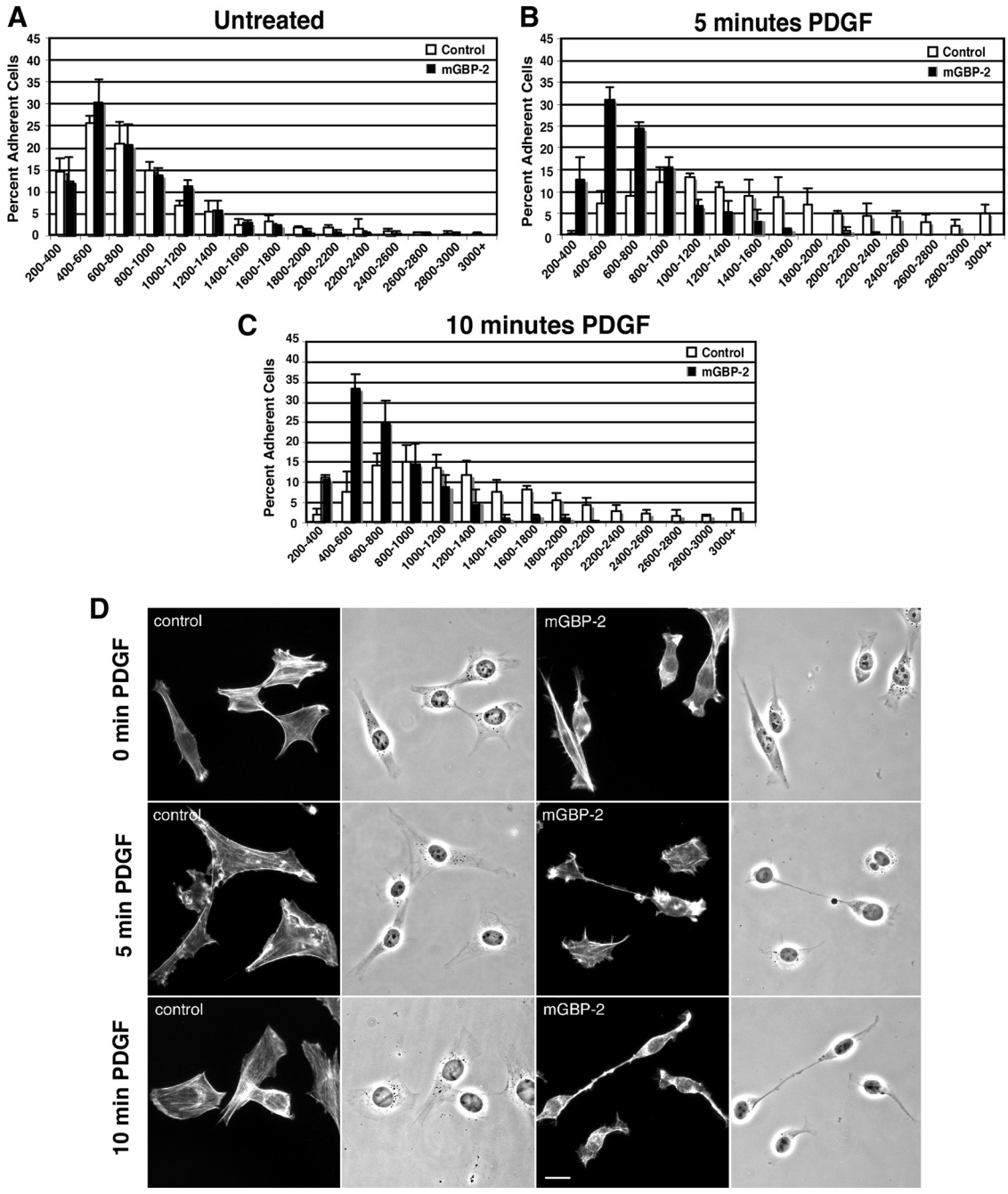

Figure 6. mGBP-2 inhibits cell spreading induced by PDGF treatment. (A) Control transfectants (empty vector) and mGBP-2–expressing cells were plated on uncoated coverslips overnight, followed by serum starvation for 2 h. Cells were treated with PDGF (10 ng/ml) for 0, 5, or 10 min. Cells were fixed, stained for Alexa 594 phalloidin, and surface areas were measured (n = 3). (B) After 5 min of PDGF treatment, surface areas were determined as described in *Materials and Methods*, and the distribution of surface areas is displayed (n = 3). (C) The surface areas of cells treated with PDGF for 10 min are shown (n = 3). (D) Fluorescent and phase images were collected of control and mGBP-2–expressing cells stained with phalloidin after PDGF (10 ng/ml) treatment for 0, 5, and 10 min. Bar, 10 μm.

S52N mGBP-2 Is Not Part of a Protein Complex Containing the p110 Subunit of PI3-K

To confirm the importance of the interaction between the p110 subunit of PI3-K and mGBP-2 to the inhibition of cell spreading, the ability of S52N mGBP-2 to interact with p110 was examined (Figure 8E). Immunoprecipitation of p110 from spreading cells demonstrated the expected interaction with mGBP-2 but S52N mGBP-2 did not interact with p110. Even at longer exposure times, no interaction was detected between S52N mGBP-2 and p110.

mGBP-2 Inhibits PI3-K Activation during Cell Spreading on FN

Control transfectants and mGBP-2–expressing cells were analyzed for PI3-K activity during cell spreading. After 2 h of serum starvation, the basal PI3-K activity in mGBP-2–

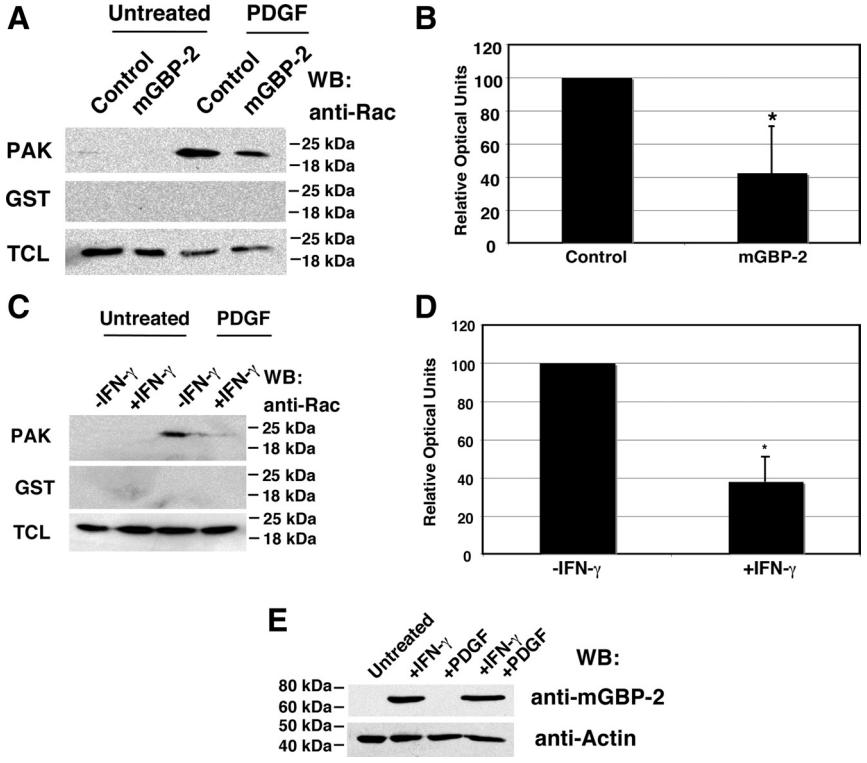

Figure 7. mGBP-2 inhibits PDGF activation of Rac. (A) Control transfectants or mGBP-2–expressing cells were serum starved for 2 h and treated with PDGF (10 ng/ml) for 5 min, harvested, and analyzed for the levels of active Rac. Western analysis of TCLs for Rac confirmed that reduced levels of active Rac are not the consequence of reduced total Rac. (B) Western blots from PBD pull-downs were quantified, and the results are expressed as described in *Materials and Methods* (*$p < 0.05$ compared with PDGF-treated control transfectants; $n = 4$). (C) Treatment with IFN-γ inhibits Rac activation by PDGF. NIH 3T3 cells were serum starved for 18 h in the presence or absence of IFN-γ (500 U/ml), treated with PDGF (10 ng/ml) for 5 min, harvested, and analyzed for the levels of active Rac. The Rac-PAK PBD/GST complexes were analyzed by Western blotting for Rac. Western analysis of TCLs for Rac confirmed that reduced levels of active Rac are not the consequence of reduced total Rac. (D) Western blots from PBD pull-downs were quantified and the results expressed as described in Figure 5 (*$p < 0.05$ compared with PDGF-treated cells that did not receive IFN [control]; $n = 4$). (E) NIH 3T3 cells were treated with 500 U/ml IFN-γ for 16 h and/or 10 ng/ml PDGF for 5 min. Cell lysates (20 μg) were analyzed for mGBP-2 expression by Western blot. The membrane was reprobed with actin to verify equal loading.

expressing cells was modestly inhibited compared with that of control transfectants (72.4 ± 3.3% of control transfectants) (Figure 9). That this could be observed when no Akt phosphorylation was observed in serum starved cells is believed to reflect the higher sensitivity of the PI3-kinase activity ELISA. Spreading of control transfectants on FN activated PI3-K significantly (157.8 ± 16.7% of control). In the presence of mGBP-2, the activation of PI3-K by spreading on FN was significantly inhibited (81.6 ± 18.6% of control). In fact, the PI3-K activity in mGBP-2 cells spreading on FN was not significantly different from that of serum-starved mGBP-2–expressing cells ($p = 0.48$).

Together, these data suggest that IFN-γ inhibits cell spreading by inhibiting Rac activation through induction of mGBP-2. This inhibition of Rac activation would be expected to slow the cytoskeletal rearrangements needed for cell spreading, consistent with our data. mGBP-2 inhibition of Rac activation is accompanied by interaction of mGBP-2 with the p110 subunit of PI3-K, a well characterized activator of Rac. Although the cellular fraction of p110 that interacts with mGBP-2 seems to be relatively small, the observation that S52N mGBP-2 neither interacts with p110 nor is able to inhibit cell spreading suggests that this interaction is physiologically significant. In fact, the presence of mGBP-2 inhibits PI3-K activation during NIH 3T3 cell spreading on FN.

DISCUSSION

Cell adhesion plays a role in normal tissue development and maintenance, as well as such processes as hematopoiesis, lymphocyte homing, and immune recruitment. It also plays a central role in disorders such as cancer, inflammation, and vascular disease. To facilitate these many processes, binding of adhesion molecules to ECM must result in the productive transduction of intracellular signals from the plasma membrane to sites as divergent as the actin cytoskeleton and the nucleus. The IFNs are involved in a variety of these processes and disorders, but their roles in influencing cell adhesion are incompletely understood.

IFNs are a family of cytokines to which many, if not most, cells are responsive (Rubinstein *et al.*, 1987). An area of IFN-mediated cellular changes that has been poorly explored is the role of IFNs in the induction of cytoskeletal changes. Although IFN treatment of some cancer cells can result in increased actin stress fiber formation and adhesion (Brouty-Boye, 1982), the opposite is observed for other cells (Hovi *et al.*, 1985). It seems that all IFN-treated cells undergo some cytoskeletal changes, but studies suggest that the cell background significantly influences these changes.

Both IFN-α/β and IFN-γ can alter cell adhesion. They do this in a variety of ways, all of which seem to show some cell type variations. In some cells, IFNs alter the expression levels of ECM proteins, thereby altering the adhesive properties of the cell's microenvironment. Whether the expression of individual components of the ECM are up- or down-regulated is very dependent on cell type (Maheshwari *et al.*, 1990; Schuger *et al.*, 1990; Diaz and Jimenez, 1997). IFNs can also influence adhesion by altering the expression levels of the receptors that mediate both ECM and cell–cell adhesion, particularly integrins. Again, these responses vary between cell types (Maruguchi *et al.*, 1991; Tsao *et al.*, 1994; Bauvois *et al.*, 1996). In addition, IFN-γ modulation of integrin-mediated adhesion in some cells does not seem to be the result of changes in levels of integrin receptors but the consequence of altering the ability of existing integrins to support adhesion. This modulation is the result of altered cytoskeletal association, phosphorylation, and reduced recruitment to focal adhesion sites (Shaw and Mercurio, 1989; Shaw *et al.*, 1990; Wills *et al.*, 1999).

One group of IFN-induced proteins for which functional information has only recently been acquired is the GBP

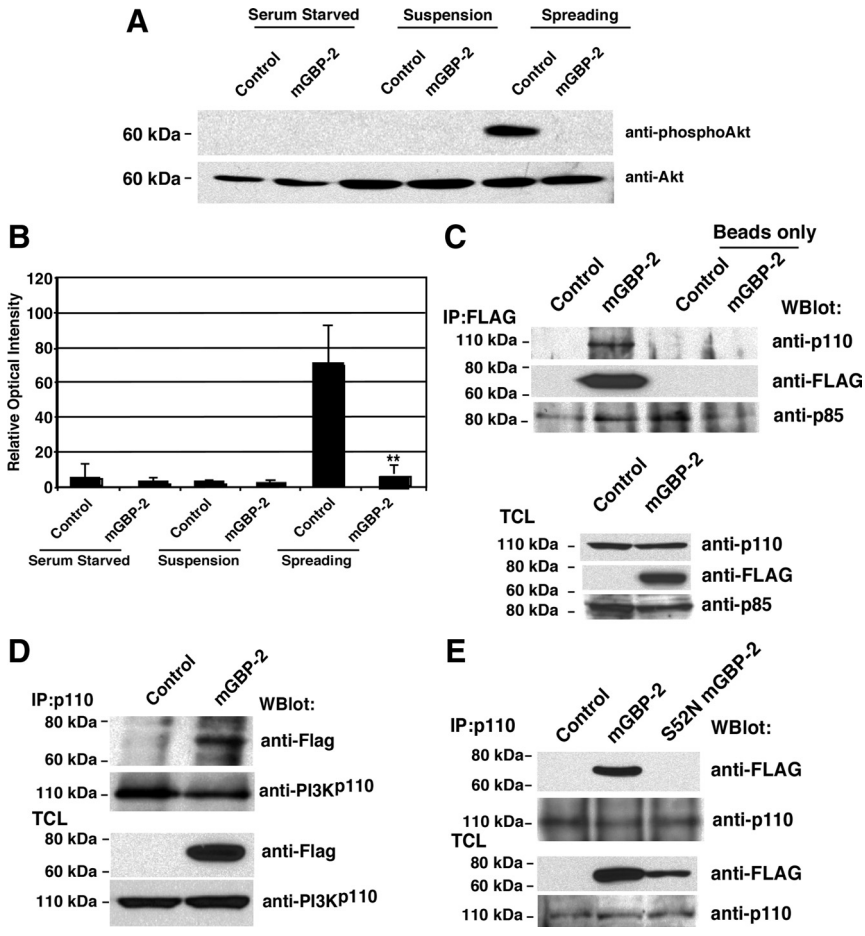

Figure 8. mGBP-2 inhibits activation of Akt and is found in a protein complex containing the p110 subunit of PI3-K. (A) Control transfectants (empty vector) and mGBP-2–expressing NIH 3T3 cells were allowed to adhere to FN-coated coverslips. Adherent cells were lysed, and cell lysates (20 μg) were size separated on 8% PAGE gels and analyzed for phospho-Akt. A representative blot shows the pAKT levels after serum starvation and before suspension (serum starved), after recovery in suspension and before plating (suspension), and after 35 min of spreading (spreading). The membrane was stripped and reprobed with antisera against Akt. (B) Western blots were quantified and the results for levels of pAkt were normalized to total cellular Akt (*$p < 0.05$ compared with control spreading cells; n = 4). (C) Control transfectant and mGBP-2–expressing cells were allowed to adhere for 35 min on FN-coated dishes. After removal of nonadherent cells by gentle washing, the adherent cells were lysed as described in *Materials and Methods*. Cell lysates (500 μg) were incubated with anti-FLAG M2 overnight at 4°C, followed by 1 h with protein G-Sepharose. Immune complexes were washed, denatured, separated on 8% PAGE gels, transferred to polyvinylidene difluoride membranes, and immunodetected with anti-p110 antibodies. Membranes were stripped and sequentially probed with rabbit anti-mGBP-2 antisera and anti-p85 antisera. TCLs (20 μg) also were included. A representative blot of three experiments is shown. (D) Cells were allowed to spread on FN-coated dishes as described and cell lysates (500 μg) were incubated with anti-p110 antibody overnight at 4°C, followed by the addition of protein G-agarose for 1 h. The immune complexes were washed and denatured, size fractionated by PAGE, and immunodetected with anti-FLAG and anti-p110 antibodies. TCLs (20 μg) also were included. Membranes were stripped and probed with rabbit anti-mGBP-2 antisera. A representative blot is shown (n = 3). (E) Control, mGBP-2–, and S52N-mGBP-2–expressing cells were allowed to spread on FN-coated dishes as described in *Materials and Methods*. Cell lysates were incubated with anti-p110 antibody overnight at 4°C followed by the addition of protein G-agarose for 1 h. The immune complexes were washed and denatured, size-fractionated by PAGE, and immunodetected with anti-FLAG antisera. Membranes were subsequently analyzed for p110. TCLs (20 μg) were included to show the level of the respective proteins. A representative blot is shown (n = 2).

family (reviewed in Vestal, 2005). They were identified almost 20 yr ago as some of the most abundantly IFN-induced proteins (Cheng *et al*., 1983, 1985). GBPs are a family of 67- to 69-kDa GTPases that are induced by both type I (α/β) and

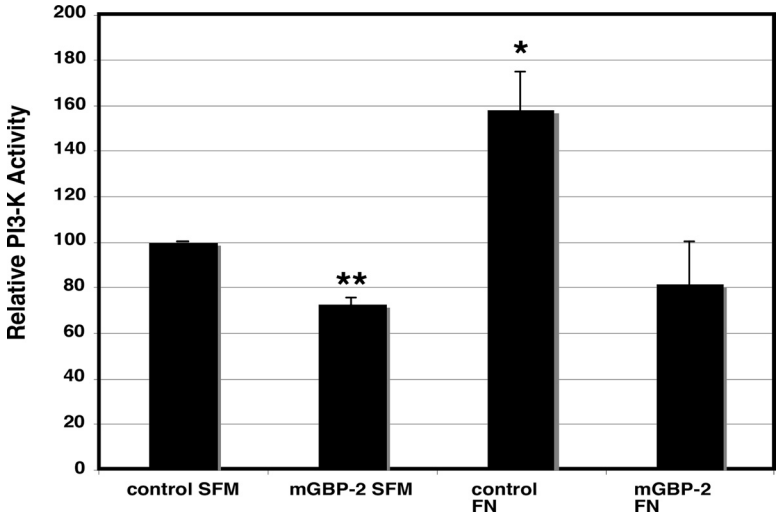

Figure 9. mGBP-2 inhibits the activation of PI3-K during cell spreading. Control transfectants and mGBP-2–expressing cells were incubated in serum-free media for 2 h (SFM) followed by processing for adhesion and spreading on FN-coated plates (FN) as described in *Materials and Methods*. After plating for 20 min on FN, cells were lysed, and PI3-K was immunoprecipitated using an antibody against p85 PI3-K. Immune complexes were used in kinase reactions and the resulting PIP_3 levels were analyzed using a PI3-kinase activity ELISA kit. The PIP_3 levels from the control transfectants after serum starvations (control SFM) for each assay were set at 100%, and all other values were normalized to the SFM control (n = 3; *$p < 0.05$, **$p < 0.01$).

type II (γ) IFNs (Cheng *et al.*, 1986; Decker *et al.*, 1991; Vestal *et al.*, 2000), as well as TNF-α and IL-1 (Cardozo *et al.*, 2001; Guenzi *et al.*, 2001). This profile of cytokines that induce GBPs suggests a role for GBPs in more generalized responses to proinflammatory cytokines. GBPs are unusual because their primary amino acid sequences contain only two of the three highly conserved consensus nucleotide binding motifs found in other GTPases (Cheng *et al.*, 1991). The third region of nucleotide contact identified for GBPs is different from that observed for other GTPases (Praefcke *et al.*, 1999; Prakash *et al.*, 2000a). Consequently, GBPs have both GDP and GMP as end products of GTP hydrolysis (Schwemmle and Staeheli, 1994; Neun *et al.*, 1996; Schwemmle *et al.*, 1996). Several members of this protein family also have a CaaX sequence at their extreme carboxy termini. CaaX sites are potentially involved in the recruitment of isoprenyl transferases that are responsible for the attachment of either C-15 farnesyl or C-20 geranylgeranyl isoprenoids to the C (cysteine) of the CaaX site (Casey and Seabra, 1996). Several of the GBPs have been shown to be isoprenylated in vivo (Nantais *et al.*, 1996; Vestal *et al.*, 1996, 1998; Stickney and Buss, 2000).

Despite the observation that one of the murine GBPs, mGBP-2, is robustly induced after IFN-γ treatment (Boehm *et al.*, 1998), almost nothing was known about the role of these proteins in mediating IFN responses until recently. Our initial discovery that the IFN-induced GTPase mGBP-2 could inhibit cell adhesion and spreading (Figure 1) suggests that we have identified a new mechanism by which IFN-γ could modulate interaction of cells with their extracellular environment. Because Rac controls lamellipodia formation in cells as they spread, we asked whether mGBP-2 inhibited Rac activity during cell spreading on FN (Figure 4). The reduction in active Rac facilitated by mGBP-2 would be expected to slow rearrangement of the actin cytoskeleton and consequently slow shape change. Depending on where in the pathways leading to Rac activation this inhibition occurs, the slowing of shape changes could be common to more than one external signal. The observation that cell spreading is inhibited by mGBP-2 on more than one matrix molecule and that adhesion is reduced on uncoated tissue culture dishes (data not shown) suggested that mGBP-2 inhibits a pathway to Rac activation that is common to multiple stimuli and is not the result of the inhibition of signals from a single integrin. This was confirmed when mGBP-2 was demonstrated to inhibit Rac activation by PDGF (Figure 7).

PI3-K is activated by almost all integrins, growth factor and cytokine receptors, and some G protein-coupled receptors (Vanhaesebroeck *et al.*, 1997; Ballou *et al.*, 2003; Welch *et al.*, 2003). The best studied of the class I PI3-K enzymes is a heterodimer containing the regulatory subunit p85 and the catalytic subunit p110 (Vanhaesebroeck *et al.*, 1997). Activation can be facilitated by the binding of the SH2 domain of the p85 regulatory subunit to tyrosine-phosphorylated residues on receptors or associated molecules and recruitment of the p85/p110 dimer to the membrane (Vanhaesebroeck *et al.*, 1997; Cantrell, 2001). Members of the Rho family (Rac and Cdc42) also can bind to p85 and contribute to PI3-K activation (Chan *et al.*, 2002; Wu *et al.*, 2007). In addition, GTP-bound Ras can bind to the p110 catalytic subunit (Rodriquez-Viciana *et al.*, 1996; Vanhaesebroeck *et al.*, 1997). PI3-K can then activate Rac by several mechanisms (Fleming *et al.*, 2000; Innocenti *et al.*, 2003; Welch *et al.*, 2003). The finding that mGBP-2 is found within a protein complex containing the p110 subunit of PI3-K suggested that mGBP-2 might inhibit PI3-K activity as a consequence of this interaction (Figure 8). Consistent with this conclusion, S52N mGBP-2, which is not found within a complex containing p110, is unable to inhibit cell spreading (Figure 8). In fact, mGBP-2 inhibits PI3-K activation during cell spreading on FN (Figure 9). Inhibiting PI3-K by binding to the p110 subunit also has been observed for activated $G\alpha_q$, which displaces Ras when it binds (Ballou *et al.*, 2003, 2006). Future studies will determine whether mGBP-2 binds directly to p110 and the significance of mGBP-2 binding to p110 to PI3-K activity.

Rac and PI3-K are both activated rapidly after binding of either type I or type II IFNs to their respective receptors (reviewed in Platanias, 2005). They are also important in signaling initiated by a wide variety of growth factors, cytokines, G protein-coupled receptors, and integrins. This study provides evidence of a novel mechanism for IFN-γ–mediated modulation of intracellular signals that impact how cells interact with their extracellular environment. IFN-γ exposure for times sufficient to induce the expression of mGBP-2 can inhibit subsequent Rac activation by cell spreading on FN or PDGF treatment. Further experiments will determine whether this reflects a more global method to inhibit signals from integrins and growth factors.

ACKNOWLEDGMENTS

We thank Drs. Judith Drazba, Amit Vasanji, and Andrea Kalinoski for assistance with image analysis. We are grateful to Drs. Ulla Knaus and Maria Diakanova for helpful discussions about the PAK pull-downs and to Dr. Fan Dong for helpful comments on the manuscript. This work was supported by American Cancer Society grant RPG-CIM-88031 (to D.J.V.).

REFERENCES

Abdullah, N., Srinivasan, B., Modiano, N., Cresswell, P., and Sau, A. K. (2009). Role of individual domains and identification of internal gap in human guanylate binding protein-1. J. Mol. Biol. *368*, 690–703.

Abramovici, H., Mojtabaie, P., Parks, R. J., Zhong, X.-P., Koretzky, G. A., Topham, M. K., and Gee, S. H. (2009). Diacylglycerol kinase ζ regulates actin cytoskeleton reorganization through dissociation of Rac1 from RhoGDI. Mol. Biol. Cell *20*, 2049–2059.

Adelmann-Grill, B. C., Hein, R., Wach, F., and Krieg, T. (1987). Inhibition of fibroblast chemotaxis by recombinant human interferon γ and interferon α. J. Cell Physiol. *130*, 270–275.

Anderson, S. L., Carton, J. M., Lou, J., Xing, L., and Rubin, B. Y. (1999). Interferon-induced guanylate binding protein-1 (GBP-1) mediates an antiviral effect against vesicular stomatitis virus and encephalomyocarditis virus. Virology *256*, 8–14.

Balasubramanian, S., Nada, S., and Vestal, D. (2006). The interferon-induced GTPase, mGBP-2, confers resistance to paclitaxel-induced cytotoxicity without inhibiting multinucleation. Cell. Mol. Biol. *52*, 43–49.

Ballou, L. M., Chattopadhyay, M., Li, Y., Scarlata, S., and Lin, R. Z. (2006). $G\alpha_q$ binds to p110α/p85α phoshoinositide 3-kinase and displaces Ras. Biochem. J. *394*, 557–562.

Ballou, L. M., Lin, H.-Y., Fan, G., Jiang, Y.-P., and Lin, R. Z. (2003). Activated $G\alpha_q$ inhibits p110α phosphatidylinositol 3-kinase and Akt. J. Biol. Chem. *278*, 23472–23479.

Bauvois, B., Van Weyenbergh, J., Rouillard, D., and Wietzerbin, J. (1996). TGF-β1-stimulated adhesion of human mononuclear phagocytes to fibronectin and laminin is abolished by IFN-γ: dependence on α5β1 and β2 integrins. Exp. Cell Res. *222*, 209–217.

Bekpen, C., Hunn, J. P., Rohde, C., Parvanova, I., Guethlein, L., Dunn, D. M., Glowalla, E., Leptin, M., and Howard, J. C. (2005). The interferon-inducible p47 (IRG) GTPases in vertebrates: loss of the cell autonomous resistance mechanism in the human lineage. Genome Biol. *6*, R92.

Berrier, A. L., Mastrangelo, A. M., Downward, J., Ginsberg, M., and LaFlamme, S. E. (2000). Activated R-Ras, Rac1, PI 3-kinase and PKCstraight-epsilon can each restore cell spreading inhibited by isolated integrin beta1 cytoplasmic domains. J. Cell Biol. *151*, 1549–1560.

Boehm, U., Guethlein, L., Klamp, T., Ozbek, K., Schaub, A., Futterer, A., Pfeffer, K., and Howard, J. C. (1998). Two families of GTPases dominate the complex cellular response to IFN-γ. J. Immunol. *161*, 6715–6723.

Boehm, U., Klamp, T., Groot, M., and Howard, J. C. (1997). Cellular responses to interferon-γ. Annu. Rev. Immunol. *15*, 749–795.

Bokoch, G. M., Vlahos, C. J., Wang, Y., Knaus, U. G., and Traynor-Kaplan, A. E. (1996). Rac GTPase interacts specifically with phosphatidylinositol 3-kinase. Biochem. J. *315*, 775–779.

Brouty-Boye, D. (1982). Interferon and reversion of the transformed phenotype. Surv. Immunol. Res. *1*, 316–322.

Cantrell, D. A. (2001). Phosphoinositide 3-kinase signalling pathways. J. Cell Sci. *114*, 1439–1445.

Cardozo, A. K., Heimberg, H., Heremans, Y., Leeman, R., Kutlu, B., Kruhoffer, M., Orntoft, T., and Eizirik, D. L. (2001). A comprehensive analysis of cytokine-induced and NF-κB dependent genes in primary rat pancreatic β-cells. J. Biol. Chem. *276*, 48879–48886.

Carter, C. C., Gorbacheva, V. Y., and Vestal, D. J. (2005). Inhibition of VSV and EMCV replication by the interferon-induced GTPase, mGBP-2, differential requirement for wild-type GTP binding domain. Arch. Virol. *150*, 1213–1220.

Casey, P. J., and Seabra, M. C. (1996). Protein prenyltransferases. J. Biol. Chem. *271*, 5289–5292.

Chan, T. O., Rodeck, U., Chan, A. M., Kimmelman, A. C., Rittenhouse, S. E., JPanayotou, G., and Tsichlis, P. N. (2002). Small GTPases and tyrosine kinases coregulate a molecular switch in the phosphoinositide 3-kinase regulatory subunit. Cancer Cell *1*, 181–191.

Cheng, Y.-S.E., Becker-Manley, M. F., Chow, T. P., and Horan, D. C. (1985). Affinity purification of an interferon-induced human guanylate-binding protein and its characterization. J. Biol. Chem. *260*, 15834–15839.

Cheng, Y. E., Colonno, R. J., and Yin Fay, H. (1983). Interferon induction of fibroblast proteins with guanylate binding activity. J. Biol. Chem. *258*, 7746–7750.

Cheng, Y. S., Becker-Manley, M. F., Nguyen, T. D., DeGrado, W. F., and Jonak, G. J. (1986). Nonidentical induction of the guanylate binding protein and the 56K protein by type I and type II interferons. J. Interferon Res. *6*, 417–427.

Cheng, Y. S., Patterson, C. E., and Staeheli, P. (1991). Interferon-induced guanylate-binding proteins lack an N(T)KXD consensus motif and bind GMP in addition to GDP and GTP. Mol. Cell. Biol. *11*, 4717–4725.

Coppolino, M. G., and Dedhar, S. (2000). Bi-directional signal transduction by integrin receptors. Int. J. Biochem. Cell Biol. *32*, 171–188.

Decker, T., Lew, D. J., and Darnell, J. E., Jr. (1991). Two distinct alpha-interferon-dependent signal transduction pathways may contribute to activation of transcription of the guanylate-binding protein gene. Mol. Cell. Biol. *11*, 5147–5153.

Degrandi, D., Konermann, C., Beuter-Gunia, C., Kresse, A., Wurthner, J., Kurig, S., Beer, S., and Pfeffer, K. (2007). Extensive characterization of IFN-induced GTPases mGTP1 to mGBP10 involved in host defense. J. Immunol. *179*, 7729–7740.

Der, S. D., Zhou, A., Williams, B.R.G., and Silverman, R. H. (1998). Identification of genes differentially regulated by interferon α, β, or γ using oligonucleotide arrays. Proc. Natl. Acad. Sci. USA *95*, 15623–15628.

Diaz, A., and Jimenez, S. A. (1997). Interferon-gamma regulates collagen and fibronectin gene expression by transcriptional and post-transcriptional mechanisms. Int. J. Biochem. Cell Biol. *29*, 251–260.

Duan, Z., Foster, R., Brakora, K. A., Yusuf, R. Z., and Seiden, M. V. (2005). GBP1 overexpression is associated with a paclitaxel resistance phenotype. Cancer Chemother. Pharmacol. *57*, 25–33.

Feig, L. A. (1999). Tools of the trade: use of dominant-inhibitory mutants of Ras-family GTPases. Nat. Cell Biol. *1*, E25–E27.

Fleming, I. N., Gray, A., and Downes, C. P. (2000). Regulation of the Rac1-specific exchange factor Tiam1 involves both phosphoinositide 3-kinase-dependent and -independent components. Biochem. J. *351*, 173–182.

Ghosh, A., Praefcke, C. J., Renault, L., Wittinghofer, A., and Herrmann, C. (2006). How guanylate-binding proteins achieve assembly stimulated processive cleavage of GTP to GMP. Nature *440*, 101–104.

Gonzalez-Amaro, R., and Sanchez-Madrid, F. (1999). Cell adhesion molecules: selectins and integrins. Crit. Rev. Immunol. *19*, 389–429.

Gorbacheva, V. Y., Lindner, D., Sen, G. C., and Vestal, D. J. (2002). The IFN-induced GTPase, mGBP-2, Role in IFN-γ induced murine fibroblast proliferation. J. Biol. Chem. *277*, 6080–6087.

Guenzi, E., *et al*. (2001). The helical domain of GBP-1 mediates the inhibition of endothelial cell proliferation by inflammatory cytokines. EMBO J. *20*, 5568–5577.

Guenzi, E., Topolt, K., Lubeseder-Martellato, C., Jorg, A., Naschberger, E., Benelli, R., Albini, A., and Sturzl, M. (2003). The guanylate binding protein-1 GTPase controls the invasive and angiogenic capability of endothelial cells through inhibition of MMP-1 expression. EMBO J. *22*, 3772–3782.

Hall, A. (1998). Rho GTPases and the actin cytoskeleton. Science *279*, 509–514.

Hermanto, U., Zong, C. S., Li, W., and Wang, L.-H. (2002). RACK1, an insulin-like growth factor I (IGF-I) receptor-interacting protein, modulates IGF-I-dependent integrin signaling and promotes cell spreading and contact with extracellular matrix. Mol. Cell. Biol. *22*, 2345–2365.

Hovi, T., Lehto, V., and Virtanen, I. (1985). Interferon affects the formation of adhesion plaques in human monocyte cultures. Exp. Cell Res. *159*, 305–312.

Innocenti, M., Frittoli, E., Ponzanelli, I., Falck, J. R., Brachmann, S. M., DeFiore, P. P., and Scita, G. (2003). Phosphoinositide 3-kinase activates Rac by entering in a complex with Eps8, Abi1, and Sos-1. J. Cell Biol. *160*, 17–23.

Itsui, Y., *et al*. (2006). Expressional screening of interferon-stimulated genes for antiviral activity against hepatitis C virus replication. J. Viral Hepatitis *13*, 690–700.

James, M. F., Beauchamp, R. L., Manchanda, N., Kazlauskas, A., and Ramesh, V. (2004). A NHERF binding site links the bPDGFR to the cytoskeleton and regulates cell spreading and migration. J. Cell Sci. *117*, 2951–2961.

Kunzelman, S., Praefcke, G.J.K., and Herrmann, C. (2005). Nucleotide binding and self-stimulated GTPase activity on human guanylate-binding protein 1 (hGBP-1). Methods Enzymol. *404*, 512–527.

Lasunskaia, E. B., Campos, M.N.N., de Andrade, M.R.M., DaMatta, R. A., Kipnis, T. L., Einicker-Lamas, M., and Da Silva, W. D. (2006). Mycobacteria directly induce cytoskeletal rearrangements for macrophage spreading and polarization through TLR2-dependent PI3K signaling. J. Leukoc. Biol. *80*, 1480–1490.

Maheshwari, R. K., Kedar, V. P., Bhartiya, D., Coon, H. C., and Kang, Y.-H. (1990). Interferon enhances fibronectin expression in various cell types. J. Biol. Regul. Homeost. Agents *4*, 117–124.

Maruguchi, Y., Toda, K.-I., Watanabe, Y., and Imamura, S. (1991). Modulatory effect of interferon-γ on the fibronectin receptor function of squamous cell carcinoma cells in vitro. J. Dermatol. Sci. *2*, 422–427.

Mira, J. P., Benard, V., Groffen, J., Sanders, L. C., and Knaus, U. G. (2000). Endogenous, hyperactive Rac3 controls proliferation of breast cancer cells by a p21-activated kinase-dependent pathway. Proc. Natl. Acad. Sci. USA *97*, 185–189.

Nantais, D. E., Schwemmle, M., Stickney, J. T., Vestal, D. J., and Buss, J. E. (1996). Prenylation of an Interferon-γ-induced GTP-binding protein: the human guanylate binding protein, huGBP-1. J. Leukoc. Biol. *60*, 423–431.

Naschberger, E., Lugeseder-Martellato, C., Meyer, N., Gessner, R., Kremmer, E., Gessner, A., and Sturzl, M. (2006). Human guanylate-binding protein-1 is a secreted GTPase present in increased concentrations in the cerebrospinal fluid of patients with bacterial meningitis. Am. J. Pathol. *169*, 1088–1098.

Neun, R., Richter, M. F., Staeheli, P., and Schwemmle, M. (1996). GTPase properties of the interferon-induced human guanylate-binding protein 2. FEBS Lett. *390*, 69–72.

Olszewski, M. A., Gray, J., and Vestal, D. J. (2006). In silico genomic analysis of the human and murine guanylate binding protein (GBP) gene clusters. J. Interferon Cytokine Res. *26*, 328–352.

Petroll, W. M., Ma, L., Kim, A., Ly, L., and Vishwanath, M. (2008). Dynamic assessment of fibroblast mechanical activity during Rac-induced cell spreading in 3-D culture. J. Cell Physiol. *217*, 162–171.

Pfeffer, L. M., Wang, E., and Tamm, I. (1980). Interferon effects on microfilament organization, cellular fibronectin distribution, and cell motility in human fibroblasts. J. Cell Biol. *85*, 9–17.

Platanias, L. C. (2005). Mechanisms of type-I- and type-II-interferon-mediated signaling. Nat. Rev. *5*, 375–386.

Praefcke, G.J.K., Geyer, M., Schwemmle, M., Kalbitzer, H. R., and Herrmann, C. (1999). Nucleotide-binding characteristics of human guanylate-binding protein 1 (hGBP-1) and identification of the third GTP-binding motif. J. Mol. Biol. *292*, 321–332.

Praefcke, G.J.K., Kloep, S., Benscheid, U., Lillie, H., Prakash, B., and Herrmann, C. (2004). Identification of residues in the human guanylate-binding protein 1 critical for nucleotide binding and cooperative GTP hydrolysis. J. Mol. Biol. *344*, 257–269.

Prakash, B., Praefcke, G.J.K., Renault, L., Wittinghofer, A., and Herrmann, C. (2000a). Structure of human guanylate-binding protein 1 representing a unique class of GTP-binding proteins. Nature *403*, 567–571.

Prakash, B., Renault, L., Praefcke, G.J.K., Herrmann, C., and Wittinghofer, A. (2000b). Triphosphate structure of guanylate-binding protein 1 and implications for nucleotide binding and GTPase mechanism. EMBO J. *19*, 4555–4564.

Price, L. S., Leng, J., Schwartz, M. A., and Bokoch, G. M. (1998). Activation of Rac and Cdc42 by integrins mediates cell spreading. Mol. Biol. Cell *9*, 1863–1871.

Qian, Y., Zhong, X., Flynn, D. C., Zheng, J. Z., Qiao, M., Wu, C., Dedhar, S., Shi, X., and Jiang, B.-H. (2005). ILK mediates actin filament rearrangements and cell migration and invasion through PI3K/Akt/Rac1 signaling. Oncogene *24*, 3154–3165.

Ridley, A. (2000). Rho GTPases: integrating integrin signaling. J. Cell Biol. *150*, F107–F109.

Rodriquez-Viciana, P., Warne, P. H., Vanhaesebroeck, B., Waterfield, M. D., and Downward, J. (1996). Activation of phosphoinositide 3-kinase by interaction with Ras and by point mutation. EMBO J. *15*, 2442–2451.

Rubinstein, M., Novick, D., and Fischer, D. G. (1987). The human interferon-γ receptor system. Immunol. Rev. *97*, 29–34.

Rupper, A. C., and Cardelli, J. A. (2008). Induction of Guanylate Binding Protein 5 by gamma interferon increases susceptibility to *Salmonella enterica* serovar typhimurium-induced pyroptosis in RAW 264.7 cells. Infect. Immun. *76*, 2304–2315.

Schnoor, M., Betanzos, A., Weber, D. A., and Parkos, C. A. (2009). Guanylate-binding protein-1 is expressed at tight junctions of intestinal epithelial cells in response to interferon-γ and regulates barrier function through effects on apoptosis. Mucosal Immunol. *2*, 33–42.

Schuger, L., Dixit, V. M., Carey, T. E., and Varani, J. (1990). Modulation of squamous carcinoma cell growth, morphology, adhesiveness and extracellular matrix production by interferon-γ and tumor necrosis factor-α. Pathobiology *58*, 279–286.

Schwartz, M. A. (2004). Rho signaling at a glance. J. Cell Sci. *117*, 5357–5458.

Schwemmle, M., Kaspers, B., Irion, A., Staeheli, P., and Schultz, U. (1996). Chicken guanylate-binding protein. Conservation of GTPase activity and induction by cytokines. J. Biol. Chem. *271*, 10304–10308.

Schwemmle, M., and Staeheli, P. (1994). The interferon-induced 67-kDa guanylate-binding protein (hGBP1) is a GTPase that converts GTP to GMP. J. Biol. Chem. *269*, 11299–11305.

Shaw, L. M., and Mercurio, A. M. (1989). Interferon γ and lipopolysaccharide promote macrophage adherence to basement membrane glycoproteins. J. Exp. Med. *169*, 303–308.

Shaw, L. M., Messier, J. M., and Mercurio, A. M. (1990). The activation dependent adhesion of macrophages to laminin involved cytoskeletal anchoring and phosphorylation of the $\alpha_6\beta_1$ integrin. J. Cell Biol. *110*, 2167–2174.

Small, J. V., Rottner, K., and Kaverina, I. (1999). Functional design in the actin cytoskeleton. Curr. Opin. Cell Biol. *11*, 54–60.

Stark, G. R., Kerr, I. A., Williams, B.R.G., Silverman, R. H., and Schreiber, R. D. (1998). How cells respond to interferons. Annu. Rev. Biochem. *67*, 227–264.

Stickney, J. T., and Buss, J. E. (2000). Murine guanylate-binding protein: incomplete geranylgeranyl isoprenoid modification of an interferon-γ-inducible guanosine triphosphate-binding protein. Mol. Biol. Cell *11*, 2191–2200.

Symes, K., and Mercola, M. (1996). Embryonic mesoderm cells spread in response to platelet-derived growth factor and signaling by phosphatidylinositol 3-kinase. Proc. Natl. Acad. Sci. USA *93*, 9641–9644.

Tsao, T.C.-Y., Xia, W., Rodberg, G. M., Pinto, C. E., and Kradin, R. L. (1994). Interferon-gamma and tumor necrosis factor-alpha promote the binding of dendritic cells to fibronectin. Pathobiology *62*, 120–126.

Vanhaesebroeck, B., Leevers, S. J., Panayotou, G., and Waterfield, M. D. (1997). Phosphoinositide 3-kinases: a conserved family of signal transducers. Trends Biochem. Sci. *22*, 267–272.

Vestal, D. J. (2005). The guanylate binding proteins (GBPs): pro-inflammatory cytokine-induced members of the dynamin superfamily with unique GTPase activity. J. Interferon Cytokine Res. *25*, 435–443.

Vestal, D. J., Buss, J. E., Kelner, G. S., Maciejewski, D., Asundi, V. K., and Maki, R. A. (1996). Rat p67 GBP is induced by interferon-gamma and isoprenoid-modified in macrophages. Biochem. Biophys. Res. Commun. *224*, 528–534.

Vestal, D. J., Buss, J. E., McKercher, S. R., Jenkins, N. A., Copeland, N. G., Kelner, G. S., Asundi, V. K., and Maki, R. A. (1998). Murine GBP-2, a new IFN-γ-induced member of the GBP family of GTPases isolated from macrophages. J. Interferon Cytokine Res. *18*, 977–985.

Vestal, D. J., Gorbacheva, V. Y., and Sen, G. C. (2000). Different subcellular localizations for the related interferon-induced GTPases, mGBP-1 and mGBP-2, implications for different functions? J. Interferon Cytokine Res. *20*, 991–1000.

Weinlander, K., Naschberger, E., Lehmann, M. H., Tripal, P., Paster, W., Stockinger, H., Hohenadl, C., and Sturzl, M. (2008). Guanylate binding protein-1 inhibits spreading and migration of endothelial cells through induction of integrin a_4 expression. FASEB J. *22*, 4168–4178.

Welch, H.C.E., Coadwell, W. J., Stephens, L. R., and Hawkins, P. T. (2003). Phosphoinositide 3-kinase-dependent activation of Rac. FEBS Lett. *546*, 93–97.

Wennstrom, S., Hawkins, P., Cooke, F., Hara, K., Yonezawa, K., Kasuga, M., Jackson, T., Cleasson-Welsh, L., and Stephens, L. (1994). Activation of phosphoinositide 3-kinase is required for PDGF-stimulated membrane ruffling. Curr. Biol. *4*, 385–393.

Wills, F. L., Gilchrist, M., and Befus, A. D. (1999). Interferon-gamma regulates the interaction of RBL-2H3 cells with fibronectin through production of nitric oxide. Immunology *97*, 481–489.

Wu, H., Yan, Y., and Backer, J. M. (2007). Regulation of class IA PI3Ks. Biochem. Soc. Trans. *35*, 242–244.

Zhang, Z.-G., Lambert, C. A., Servotte, S., Chometon, G., Eckes, B., Krieg, T., Lapiere, C. M., Nusgens, B. V., and Aumailley, M. (2006). Effects of constitutively active GTPases on fibroblast behavior. Cell. Mol. Life Sci. *63*, 82–91.